博士論文

Alternative epigenetic modification of tumor microenvironment by differentially spliced YAP1 isoforms

（YAP1 のスプライスアイソフォーム依存的な

腫瘍微小環境のエピジェネティック修飾変動）

武 暁婧

Wu Xiaojing

Index

Abstract

YAP1 is a prooncogenic transcriptional coactivator that is negatively regulated by the tumor-suppressive Hippo signaling pathway. YAP1 comprises two major splicing isoforms, YAP1-2α and YAP1-2γ, which lack and possess the γ-segment that disrupts the leucine zipper, respectively. YAP1-2α, but not YAP1-2γ, stimulates nuclear translocalization of the oncogenic tyrosine phosphatase SHP2 upon complex formation via the leucine zipper.

YAP1-2γ, which is primarily localized to the cytoplasm, exhibits stronger cell-intrinsic prooncogenic activity because cytoplasmically retained SHP2, due to the lack of YAP1-2γ, potentiates RAS–ERK signaling, thereby promoting cell proliferation and motility. In striking contrast to the *in vitro* observations, YAP1-2γ confers less strong tumorigenicity than YAP1-2α *in vivo*. Mechanistically, under hypoxic conditions *in vivo,* YAP1-2γ transactivates the *Ccl2* chemokine mRNA by recruiting H3K4me3 methyltransferase Mll1 to the *Ccl2* promoter region under hypoxic condition i*n vivo*. Induction of *Ccl2* then triggers the recruitment of tumor-inhibitory M1 macrophages to the tumor lesion and consequently makes a "hot" tumor microenvironment in terms of innate immunity. In contrast, YAP1-2α functions as a

transrepressor of *Ccl2* by forming the YAP1-2α/Tead/SHP2 heterotrimeric complex, which subverts M1 macrophage accumulation and leads to a "cold" tumor microenvironment. These results indicate that alternative splicing intricately influences the cell-intrinsic and cell-extrinsic activities of YAP1 isoforms in terms of cancer development.

Introduction

Yes-associated protein 1 (YAP1), a major downstream effector of the Hippo pathway, is a crucial regulator of cell proliferation and apoptosis (1, 2). Upon stimulation of the Hippo signaling pathway, the upstream Hippo core kinase MST1/2 phosphorylates and activates the downstream Hippo core kinase LATS1/2, which in turn phosphorylates the transcriptional coactivator YAP1 and its homologue TAZ, thus enforcing cytoplasmic retention of these coactivators via the interaction with 14-3-3, followed by proteasomal degradation (3, 4). When Hippo signaling is off, inactivation of MST1/2 and LATS1/2 kinase activities liberates YAP1 and TAZ from inhibitory phosphorylation, thus causing their translocalization into the nucleus (5). As transcriptional coactivators, which do not directly bind to a particular DNA sequence, nuclear-localized YAP1/TAZ interacts with various transcription factors, most notably TEA domain family member (TEAD) transcription factors. The YAP1/TAZ-TEAD protein complex transactivates genes that regulate cell proliferation, apoptosis, and cell fate (6). Accumulating evidence indicates that YAP1/TAZ are oncogenes that are overexpressed in many human cancer types (7, 8).

The human *YAP1* gene has been shown to generate at least 8 distinct YAP1 isoforms via alternative splicing of the *YAP1* pre-mRNA. Exon 6 is an evolutionarily conserved cassette exon encoding the γ-segment comprising 16-amino-acid residues, inclusion of which disrupts the leucine zipper structure in YAP1. Exclusion of exon 6 produces the YAP1-1α, YAP1-1β, YAP1-2α, and YAP1-2β isoforms, while inclusion of exon 6 into *YAP* mRNA produces the YAP1-1γ, YAP1-1δ, YAP1-2γ, and YAP1-2δ isoforms, which does not have a functional leucine zipper due to the insertion of the γ-segment (9). Mouse *Yap1* was reported primarily comprises two isoforms: the short-form, which corresponds to human YAP1-2α, and the long-form, which corresponds to human YAP1-2γ (9, 10) (Figure 1A). In this study, I focused on the two major YAP1 isoforms, YAP1-2α and YAP1-2γ, because they are evolutionally conserved and representative YAP1 isoforms with (YAP1-2α) or without (YAP1-2γ) the functional leucine zipper.

SHP2 protein tyrosine phosphatase (PTPase), a *bona fide* oncoprotein involved in potentiating the pro-mitogenic signal activated by the RTK (receptor-tyrosine kinase)-RAS-REK pathway and its gain-of-function mutations have been associated with several types of cancer (11).

Deregulation of SHP2 by the *Helicobacter pylori* CagA oncoprotein is also associated with the development of gastric cancer (12). YAP1 plays an important role in translocating SHP2 from the cytoplasm to the nucleus (13) (Figure 1B). Cytoplasmic SHP2 plays a vital role in fully activating the RTK-RAS-ERK pathway (14, 15). On the other hand, nuclear SHP2 potentiates β-catenin/TCF-dependent gene expression in the Wnt signaling pathway (16). Accordingly, physical interaction of YAP1 with SHP2 is critically involved in determining the intracellular functions of the SHP2 oncoprotein. In the previous study, we investigate whether splicing variations of YAP1 affect SHP2-binding activity and found experiment revealed that YAP1-2α could interact with SHP2 in a TAZ-dependent manner (17). In contrast, YAP1-2γ, which does not have an intact leucine zipper, failed to form a complex with SHP2. Consistent with this finding, the ectopic expression of YAP1-2α translocated SHP2 into the nucleus, whereas YAP1-2γ did not (17).

Chromatin is a highly ordered structure that comprises DNA, histone, and other chromosomal proteins. The state of chromatin is affected by environmental stresses such as hypoxia, heat exposure, and DNA damage signaling cascades that evoke genetic and epigenetic modification

(18). Malfunctioning in the modification of chromatin has been widely implicated in the development of various diseases including autoimmunity and cancer as well as aging (19). Specifically, methylation status of histones is highly important because it coordinates the regulation of gene expression. Certain methylations, such as trimethylation of histone 3 at lysine 4 (H3K4me3), are present in active promoters (19). Elevated H3K4me3 and transcriptional activity have been correlated with the coactivator activity of YAP1 in several cancers, such as hepatocellular carcinoma and colorectal cancer (20, 21).

Previously, we demonstrated that YAP1-2γ confers greater *in vitro* pro-oncogenic potential to mouse non-transformed NIH3T3 fibroblasts than YAP1-2α did. Also, NIH3T3 cells expressing YAP1-2γ showed stronger mitogenic and motogenic activities, which is due to YAP1-2γ strengthened RAS-ERK signaling by retaining SHP2 in the cytoplasm.

In contrast when we subcutaneously injected the NIH3T3 transfectants that stably express HA-YAP1-2α or HA-YAP1-2γ into the flanks of the nude mice, those expressing YAP1-2α gave rise to much larger tumors compared to those expressing YAP1-2γ (17). We also found massive infiltration of macrophages in the YAP1-2γ–induced tumors but not YAP1-2α-induced tumors.

The mechanism by which YAP1-2γ–expressing NIH3T3 transfectants recruited macrophage *in vivo* was that YAP1-2γ/TEAD complex transactivated *CCL2*, a monocyte/macrophage chemoattractant, whereas YAP1-2α/TEAD/SHP2 complex repressed *CCL2* transcription (17) (Figure 1C).

To further investigate the above-described observations, *in vitro* cell lines were re-established from tumors developed by YAP1-2α–expressing NIH3T3 cells or YAP1-2γ–expressing NIH3T3 in nude mice. By analysis the characteristic difference between tumor-derived cell line and parental transfectant, we investigated the mechanism by which spliced YAP1 isoforms alter the tumor microenvironment.

Figure 1

A

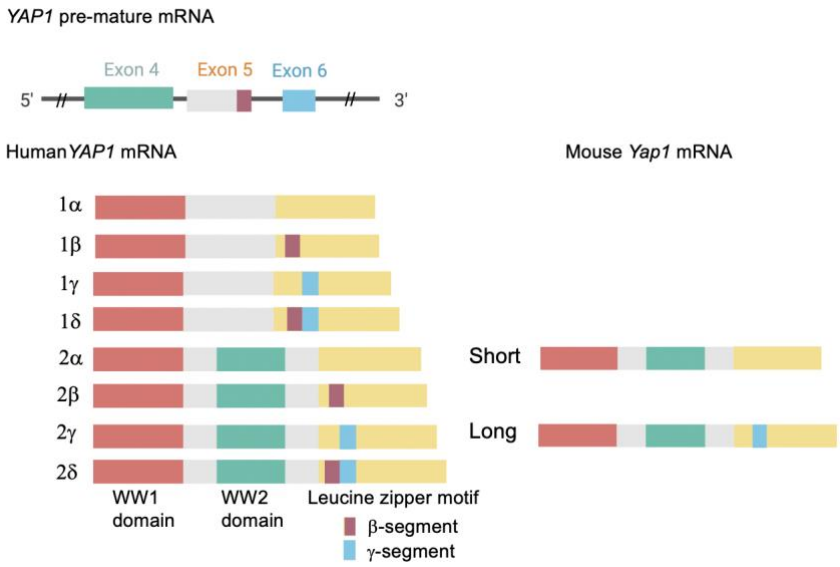
YAP1 pre-mature mRNA
Exon 4
Exon 5
Exon 6
5'
3'
Human YAP1 mRNA
Mouse Yap1 mRNA
1α
1β
1γ
1δ
2α
2β
2γ
2δ
Short
Long
WW1 domain
WW2 domain
Leucine zipper motif
β-segment
γ-segment

B

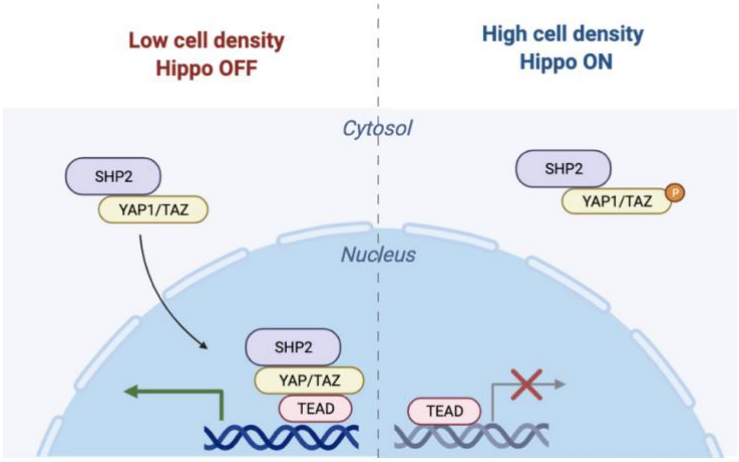
Low cell density
Hippo OFF
High cell density
Hippo ON
Cytosol
SHP2
YAP1/TAZ
SHP2
YAP1/TAZ
P
Nucleus
SHP2
YAP/TAZ
TEAD
TEAD

C

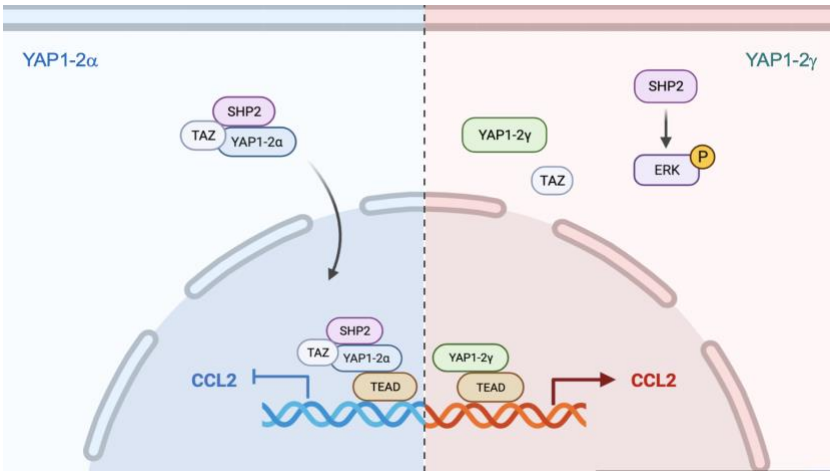

Figure 1. YAP1 isoforms and the crosstalk between YAP1 and SHP2.

A. The isoforms of human *YAP1* and mouse *Yap1*. B. YAP1 plays an important role in translocating SHP2 from the cytoplasm to the nucleus. C. YAP1-2γ/TEAD complex transactivated CCL2, whereas YAP1-2α/TEAD/SHP2 complex repressed CCL2 transcription.

Methods

Cell culture and transfection

Human gastric epithelial AGS cells were cultured at 37 °C under 5% CO_2 in RPMI medium containing 10% fetal bovine serum (FBS). HEK 293T cells and mouse embryo-derived fibroblast NIH3T3 cells were cultured at 37 °C under 5% CO_2 in DMEM medium containing 10% FBS. According to the manufacturer's instructions, DNA transfection was performed by using Lipofectamine 2000 reagent (Invitrogen). Generally, the cells were harvested at 24 hours post-transfection for analysis.

Plasmid Design and Construction

The cDNA was constructed using the mutagenesis method and cloned into the pCDH-CMVp-MCS-EF1p-*Puro* vector to make expression vectors. CRISPR/Cas9 px330 vector was used for all of the knockout experiments. The guide RNA was designed by using online tool CRISPR Genome Engineering Resources. Guide RNA sequences were shown in the sgRNA list.

sgRNA List

YAP1-sgRNA: 5’- CATCAGATCGTGCACGTCCG-3’

Yap1-sgRNA: 5’- GGCAGCTTGCGAAGCCGCAT-3’

Shp2-sgRNA: 5’- CTCCGCGGGGTACCGTCACA-3’

Taz-shRNA#1: 5’-CCTGCATTTCTGTGGCAGATA-3’

Taz-shRNA#2: 5’-CAGCCGAATCTCGCAATGAAT-3’

Establishment of the stable transfectants with lentiviral vectors

Packaging vectors (psPAX2, pMD2.G) and Lenti-X^{TM}293T cells (Takara #632180) were used for constructing lentivirus. Lentivirus titer (MOI; Multiplicity of Infection) was detected by using the Lenti-X Titration Kit (Takara). During the infection, lentivirus combined with 20 μM polybrene (SIGMA) was added to the culture medium. 4.5 μM puromycin was added into the cell culture medium to perform the positive selection at 48 hours post-infection.

Antibodies

Anti-FLAG antibody (M2, SIGMA), anti-HA antibody (C29F4, Cell Signaling Technologies), anti-YAP1 antibody (1A12, Cell Signaling Technologies), anti-SHP2 antibody (B-1, Santa Cruz), anti-SRSF3 antibody (7B4, Invitrogen Antibodies), anti-YAP1/TAZ antibody (D24E4, Cell Signaling Technologies), anti-CCL2 antibody (MABN712, Sigma-Aldrich), anti-MLL-HRX antibody（05765- Sigma-Aldrich），anti-mouse IgG antibody (D1416, Santa Cruz), anti-Rabbit IgG antibody (L2414, Santa Cruz), anti-Pan-TEAD antibody (D3F7L, Cell Signaling Technologies), anti-β-actin antibody (8H10D10, Cell Signaling Technologies); anti-CD86 antibody (bs-1035R, BIOSS), anti-CD163 antibody (EPR19518, Abcam), anti-p44/42 MAPK (Erk1/2) antibody (9102s, Cell Signaling Technologies), anti-phospho-p44/42 MAPK (Erk1/2) antibody (9101s, Cell Signaling Technologies) were used as primary antibodies for immunostaining, immunoprecipitation, chromatin immunoprecipitation, immunohistochemistry, and immunoblotting.

Immunofluorescent staining and immunohistochemical staining

Poly-*D*-lysine-coated glass cover-slips (IWAKI) was used to seed cells. After harvested, samples were fixated with 4% paraformaldehyde. Then permeabilized the fixed cells with 0.1% TritonX-100 for 10 min at room temperature and then proceeded antibody treatment. Fluorescent images were taken by using FLUOVIEW viewer software (version 4.1a, Olympus).

Tumors harvested from the nude mice were fixed in paraformaldehyde solution, fastened in paraffin for section. Sectional samples were deparaffinized, rehydrated, antigen-retrieved, and subjected to incubation with the respective antibodies. Vectastain ABC-Elite kit (Vector Laboratories) was used to stain sample sections according to the manufacturer's protocols. All the animal experiments were carried out according to the Ethics Committee for Animal Experiments protocol at the Graduate School of Medicine, The University of Tokyo.

Immunoprecipitation and immunoblotting

After harvested, cells were treated with lysis buffer (NaCl (100 mM), Tris-HCl (50 mM, pH 7.5), EDTA (5 mM), Brij35 (1%), β-glycerophosphate (1 mM), NaF (10 mM), Na_3VO_4 (2 mM)

and PMSF (2 mM), Aprotinin (2 mM), Leupeptin (2 mM), Trypsin inhibitor (2 mM)). For immunoprecipitation, protein G Sepharose 4^{TM} Fast Flow (GE Healthcare) was pre-incubated with respective antibodies. Cells lysate was incubated with tagged-beads at 4 degree overnight. The beads-protein complex was washed by using lysis buffer for 4 times, and treated with elution buffer. SDS-PAGE proteins were detected by using Western Lightning Plus ECL (Perkin-Elmer, Inc.). The chemiluminescence was exposed on the X-ray film (Fuji Film) and quantified using the LAS4000 system (Life Technologies).

RNA isolation and Quantitative RT-PCR

Total RNA from cells or tumors was treated by Trizol Regent (Ambion). 1 ug total RNA was used to perform reverse transcription with SuperScript II (Invitrogen) with the random primer (Invitrogen). After RNaseH treatment, SYBR *Premix Ex Taq* II (TaKaRa) was used to do qPCR with OnePlus RealTime PCR system (Life Technologies). ΔCt method was used to evaluate the quantity of mRNA. ΔCt was compared between sample mRNA and the endogenous reference genes. ΔΔCt was calculated as the between the sample and the control. Finally, the fold change in mRNA expression was calculated as $2^{-\Delta\Delta Ct}$.

List of the primers for RT-PCR

Human *YAP* exon 6

Forward: 5’- ATGCGGAATATCAATCCCAGCAC-3’

Reverse: 5'- CTCGAGAGTGATAGGTGCCACT-3'

Human total *YAP* mRNA

Forward: 5'- CCTTCTTCAAGCCGCCGGAG-3'

Reverse: 5’- CAGTGTCCCAGGAGAAACAGC-3’

Mouse *Yap* exon 6

Forward: 5’- ATACGGAATATCAATCCCAGCAC-3’

Reverse: 5'- CTCGAGAGTGATAGGTGCCACT-3'

Mouse total *Yap* mRNA

Forward: 5'- CCTTCTTCAAGCCGCCTGAG-3'

Reverse: 5’- GAGTGTCCCAGGAGAAACGGC-3’

Mouse *Ccl2*

Forward: 5’- TGCATCTGCCCTAAGGTCTTCA-3’

Reverse: 5’- AGTGCTTGAGGTGGTTGTGGA-3’'

Mouse *Hprt*

Forward: 5’- ACTGTAATGATCAGTCAACGGG-3’

Reverse: 5’- GGCCTGTATCCAACACTTCG-3’

Mouse 18s-Ribosomal RNA

Forward: 5'- F: GGACCAGAGCGAAAGCATTTGCC'

Reverse: 5’- TCAATCTCGGGTGGCTGAACG’

Allograft transplantation experiments

Six-week-old female athymic nude mice (BALB/c; nu/nu) were used for tumor-formation assay. Five pairs of stable NIH3T3 transfectants (pairs 1–5) that express comparable levels of YAP1-2α or YAP1-2γ were constructed. Each pair of NIH3T3 transfectant (1.5×10^6) was injected into the right or left flank in each mouse (n=5). The mice were sustained under aseptic barrier conditions until they were sacrificed at 6 weeks. All the animal experiments were performed at the Graduate School of Medicine of the University of Tokyo according to the protocol of the Ethics Committee for Animal Experiments.

Cell line derivation from Tumors

Tumors obtained from nude mice (pair 5) were treated in HBSS (Gibco) containing collagenase II (2.5 mg/ml, Worthington) and DNase (0.5 mg/ml, Worthington) at 37 ℃. The digested tissue was pipetted and centrifuged. Pellet was resuspended and plated in a culture medium DMEM.

Chromatin immunoprecipitation assay

Chromatin immunoprecipitation (ChIP) was performed with antibodies against H3K4me3, and MLL-THX using chromatin extracted from YAP1-2α–NIH3T3, YAP1-2γ–NIH3T3, YAP1-2αT, and YAP1-2γT, respectively. Firstly, cells were cross-linked with fresh 1% formaldehyde (Thermo Fisher Scientific AG) for 10 minutes at room temperature. Then 1 mM glycine (Sigma-Aldrich) was added to inactivate formaldehyde. Then cells were lysed by using lysis buffer and sheared by a sonicator to generate chromatin fragments between 200-500 base pairs; the fragment sizes were confirmed by agarose gel electrophoresis. 50 μl (25%) sheared lysate was used as input. 100 μl of Protein G beads (Invitrogen) were pre-incubated with respective antibody for 12 h at 4 degree. The lysate was subjected to perform immunoprecipitation with tagged-beads. After overnight incubation, beads were washed 2 times with ChIP dilution buffer, 1 time with wash buffer I, 1 time with wash buffer II, and 3 times with TE buffer. Protein–chromatin complexes were incubated by using elution buffer containing 1% SDS at 65◦C. Immunoprecipitated genome DNA and were further treated with RNaseA (Thermo Scientific) and proteinase K (Thermo Scientific) and extracted by phenol-chloroform method and then

purified by ethanol. The immunoprecipitated genome DNA was detected by agarose. The fold change of the enrichment was measured by qPCR.

Statistical analyses

Unpaired two-tailed Student's t-tests were used in qRT-PCR. Paired two-tailed Student's t-tests were used in the growth curve, immunohistochemical staining experiments to compare the different significance of YAP1-2α and YAP1-2γ. Kaplan-Meier curve is generated using Excel software; original data is downloaded from (The Cancer Genome Atlas) TCGA database.

Results

1. Increased expression of *Ccl2* in tumor-derived YAP1-2γT cells.

Previously, we performed allograft transplantation experiments by injecting the NIH3T3 transfectants (YAP1-2α–NIH3T3 and YAP1-2γ–NIH3T3) into the flanks of the nude mice, YAP1-2γ–NIH3T3 derived much smaller tumors compared to YAP1-2α–NIH3T3 due to macrophages infiltration. Also, the mechanism for which is YAP1-2γ/TEAD complex transcriptionally activated *CCL2* expression, whereas YAP1-2α/TEAD complex transcriptionally repressed *CCL2* expression (17). To test this finding in tumor cells passaged *in vivo*, we established *in vitro* tumor cell lines from NIH3T3 tumors developed in nude mice. The cell line established from *in vivo* passaged YAP1-2α–NIH3T3 tumor was termed the YAP1-2αT cell, and the cell line established from *in vivo* passaged YAP1-2γ–NIH3T3 tumor was termed the YAP1-2γT cell. The parental transfectants were referred to as YAP1-2α–NIH3T3 and YAP1-2γ–NIH3T3 (Figure 2A).

To compare the mitogenic activity between tumor-derived cells and parental transfectants, the growth curves were generated by calculating viable cell numbers. Consist with our previous

data that YAP1-2γ exhibits stronger mitogenic activity than YAP1-2α, YAP1-2γ–NIH3T3 grew faster than YAP1-2α–NIH3T3. However, although both tumor-derived cell lines grew faster than their parental transfectants, there was a reverse that YAP1-2αT grew faster than YAP1-2γT. Combined with the previous result that YAP1-2α confers greater *in vivo* tumorigenicity than YAP1-2γ, these data suggested that YAP1-2γT and YAP1-2αT cells maintained the tumorigenic potential when cultured *in vitro* (17) (Figure 2B).

The levels of *Ccl2* expression in tumor-derived cells were then compared with those in parental NIH3T3 transfectants. RNA-sequencing analysis showed that the *Ccl2* mRNA expression level in the YAP1-2γT cells was far greater than that in the YAP1-2αT cells (22) (Figure 2C). This result was confirmed by qRT-PCR analysis. On the other hand, the level of *Ccl2* mRNA in YAP1-2αT cells was much lower than that in the YAP1-2α–NIH3T3 (Figure 2D). These results were also confirmed at the level of Ccl2 protein expression by western blotting (Figure 2E). The conclusion of our previous study that YAP1-2γ/TEAD complex transcriptionally activates *CCL2/Ccl2* cannot fully explain the result; drastic enhancement of CCL2/Ccl2 expression by passaging NIH3T3-derived tumor cells expressing YAP1-2γT in *in vivo*.

Figure 2

A

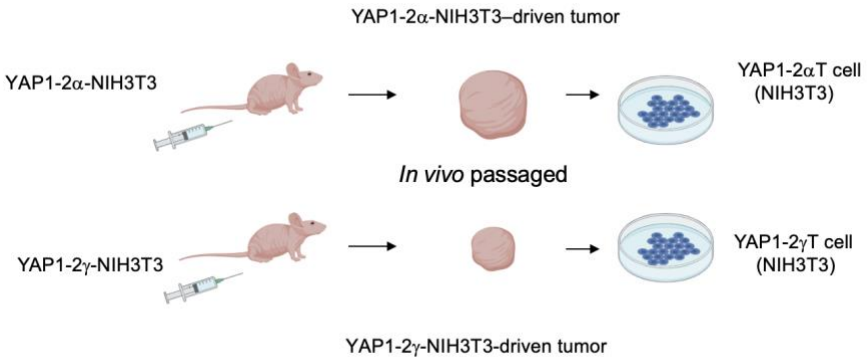

Tumor cell lines derived from NIH3T3 transfectants-driven tumors on nude mice.

B

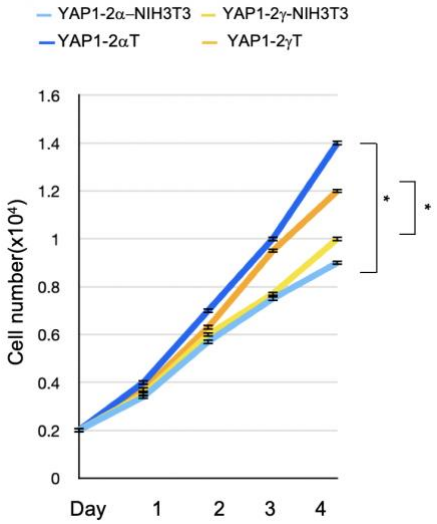

The growth curves of YAP1-2αT, YAP1-2γT, YAP1-2α–NIH3T3 and YAP1-2γ–NIH3T3.

C

RNA-seq

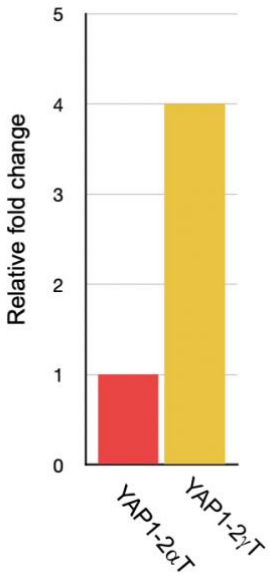

D

qRT-PCR

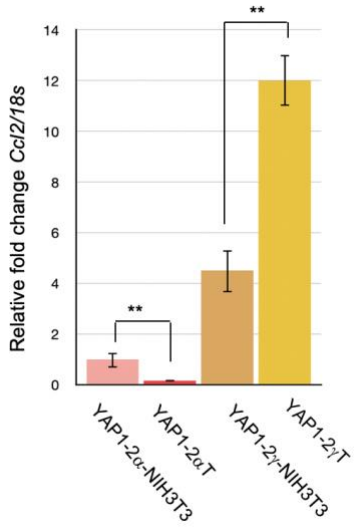

The relative mRNA expression levels of *Ccl2* in YAP1-2αT, YAP1-2γT, YAP1-2α–NIH3T3 and YAP1-2γ–NIH3T3.

E

WB

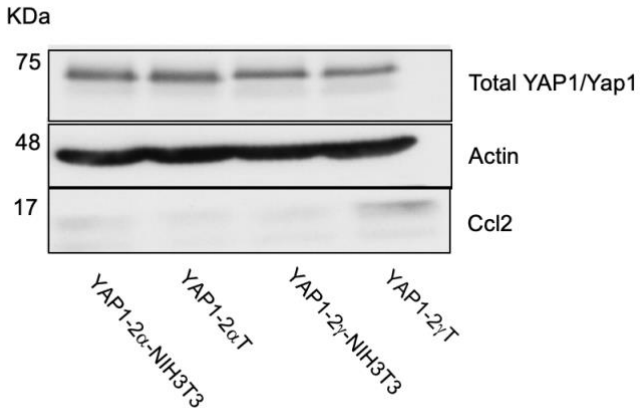

The protein expression levels of *Ccl2* in YAP1-2αT, YAP1-2γT, YAP1-2α–NIH3T3 and YAP1-2γ–NIH3T3.

Figure 2. The increased expression of the *Ccl2* mRNA in tumor-derived YAP1-2γ cells. A. Tumor cell lines derived from NIH3T3 transfectants-formed tumors on nude mice. B. The growth curves of YAP1-2αT cell and YAP1-2γT and NIH3T3 transfectants were generated by calculating viable cell numbers. Error bars represents means S.D., *: $p< 0.05$, Student's t-test. Quantitative data were obtained from three independent experiments. C. The results of RNA-Seq, the relative mRNA expression levels of *Ccl2* in YAP1-2αT and YAP1-2γT. Quantitative data were obtained from three independent experiments D. qRT-PCR analysis of *Ccl2* mRNA expression in NIH3T3 cells in YAP1-2αT cell and YAP1-2γT cells and NIH3T3 transfectants. Error bars represents mean ± S.D., *: $p< 0.05$, **: $p< 0.01$, Student's t-test. Quantitative data were obtained from three independent experiments E. The expression levels of Yap1, Ccl2, and Actin in YAP1-2αT cell, YAP1-2γT cells, and parental NIH3T3 transfectant were determined by immunoblot analysis. Cell lysates from YAP1-2αT cell, YAP1-2γT cells, and NIH3T3 transfectants were subjected to immunoblot analysis with the respective antibodies.

2. YAP1-2γT showed more specific activated promoters with enriched H3K4me3 peaks.

The methylation status of histones plays an important role in the epigenetic regulation of gene expression. Certain types of histone methylation such as trimethylation of histone 3 at lysine 4 (H3K4me3) are reported to be present in transcriptionally active promoters (19). *YAP1* is reported to act as a key regulator of the H3K4me3 modification in several cancer cells (20, 21). To test if epigenetic modifications were responsible for the higher-level expression of *Ccl2* in YAP1-2γT cells, chromatin immunoprecipitation followed by deep DNA sequencing (ChIP-seq) was performed. The ChIP-seq revealed systemic profile of H3K4me3 modification pattern in YAP1-2αT and YAP1-2γT cells.

Compared to YAP1-2αT cells, the genome of YAP1-2γT cells contained more activated promoters with significantly enriched H3K4me3 peaks (Figure 3A). A total of 4941 promoters were specifically activated in YAP1-2γT cells, whereas 279 promoters were specifically activated in YAP1-2αT cells. Motif analysis of the precipitated DNA fragments revealed that JunB, BORIS, and TEAD were mostly associated transcription factors that may transcriptionally activate gene expression in YAP1-2γT cells (23) (Figure 3B). Pathway

association analysis using the molecular signatures database (MSigDB) (24, 25) showed that genes with elevated H3K4me3 peaks exhibited a significant association of interferon response and hypoxia signaling (Figure 3C).

Figure 3

A

ChIP-seq

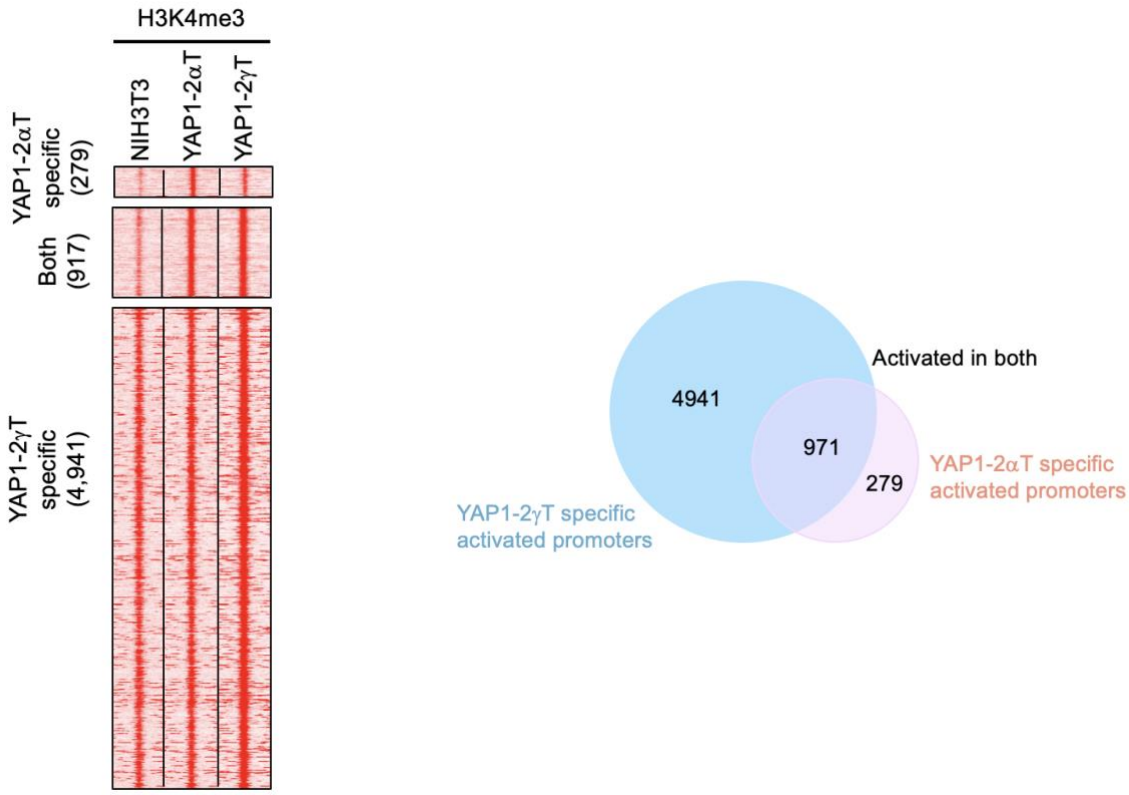

ChIP-seq analysis of NIH3T3, YAP1-2αT, and YAP1-2γT.

B

De novo motif at Yap1-2γT specific activated promoters

Rank	Motif	P-value	Best match
1		$1x10^{-224}$	JunB(bZIP)
2		$1x10^{-163}$	BORIS(Zf)
3		$1x10^{-57}$	POL003.1_GC-box
4		$1x10^{-47}$	TEAD

C

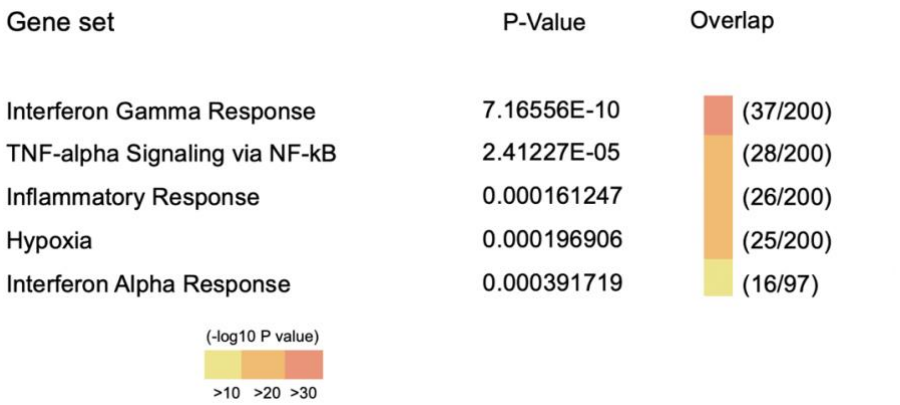

Pathway association analysis using the molecular signatures database (MSigDB)

Figure 3. YAP1-2γT showed more specific activated promoters with enriched H3K4me3 peak. A. *(left)* Distribution of the H3K4me3 signals in NIH3T3, YAP1-2αT, and YAP1-2γT cells. *(right)* Overlap of peaks in YAP1-2αT and YAP1-2γT cells. B. YAP1-2γT-specific activated promoters. C. Significant enrichment of gene set signatures (MsigDB) in YAP1-2γT cells was analyzed by Gene group association analysis.

3. Histone methyltransferase Mll1 enriched at the *Ccl2* promoter region in YAP1-2γT.

To examine whether H3K4me3 was elevated in the *Ccl2* promoter regions of in YAP1-2α–NIH3T3, YAP1-2αT, YAP1-2γ–NIH3T3, and YAP1-2γT, ChIP-qPCR experiment was performed by using an anti-H3K4me3 antibody and control anti-IgG antibody. Compared to YAP1-2γ–NIH3T3, pronounced H3K4me3 accumulation was observed in the *Ccl2* promoter region (-1040 bp/-950 bp) in YAP1-2γT. However, YAP1-2αT cells had a weaker H3K4me3 signal than that of YAP1-2α–NIH3T3 (Figure 4A). Since H3K4me3 is correlated with transcriptional activation, epigenetic modification of the *Ccl2* promoter region may be responsible for *Ccl2* hyperactivation in YAP1-2γT cells during *in vivo* passage (19).

In mammals, mixed-lineage leukemia (MLL)/SET or COMPASS family members act as methyltransferases that mediate mono-, di- or tri-methylation of H3K4 (26). Among MLL family members, MLL1 is the predominant methyltransferases for H3K4 tri-methylation, which plays important roles in tumor initiation (26). Of note, Mll1 coimmunoprecipitated Yap1 in organoids from mouse intestinal epithelium, and *vice versa*, suggest the possibility that Mll1 is responsible for elevated H3K4me3 in YAP1-2γT cells (27). MLL1 is proteolytically processed

into N-terminal p320 (N320) and C-terminal p180 (C180) fragments, the latter of which contains the histone methyltransferase domain (SET domain). The two fragments heterodimerize to form a stable complex and localize to the subnuclear compartment (28).

Given this, the level of Mll1 expression in NIH3T3 cells were examined by using an anti-Mll^{c180} antibody. As a result, there were no changes in Mll1 expression between parental and tumor derived NIH3T3 cells (Figure 4B). Since histone methylation requires the recruitment of methyltransferases to the methylation site, ChIP-qPCR was performed using the anti-Mll^{c180} antibody.

The enrichment of Mll1 showed no difference between YAP1-2α–NIH3T3 and YAP1-2αT cells. However, compared with YAP1-2γ–NIH3T3, YAP1-2γT cells exhibited a greater Mll1 signal on the *Ccl2* promoter region, suggesting that YAP1-2γT has an ability to recruit the methyltransferase to specific promoter legions including the *Ccl2* promoter (Figure 4C).

Figure 4

A

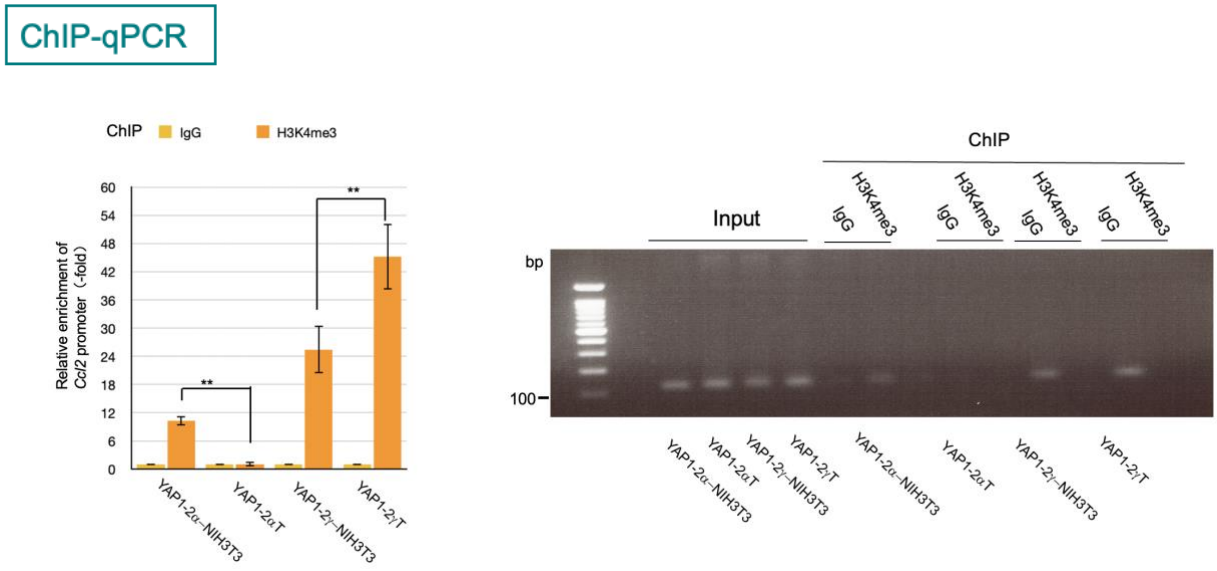

The ChIP analysis (anti-H3K4me3) of YAP1-2αT, YAP1-2γT, YAP1-2α–NIH3T3 and YAP1-2γ–NIH3T3.

B

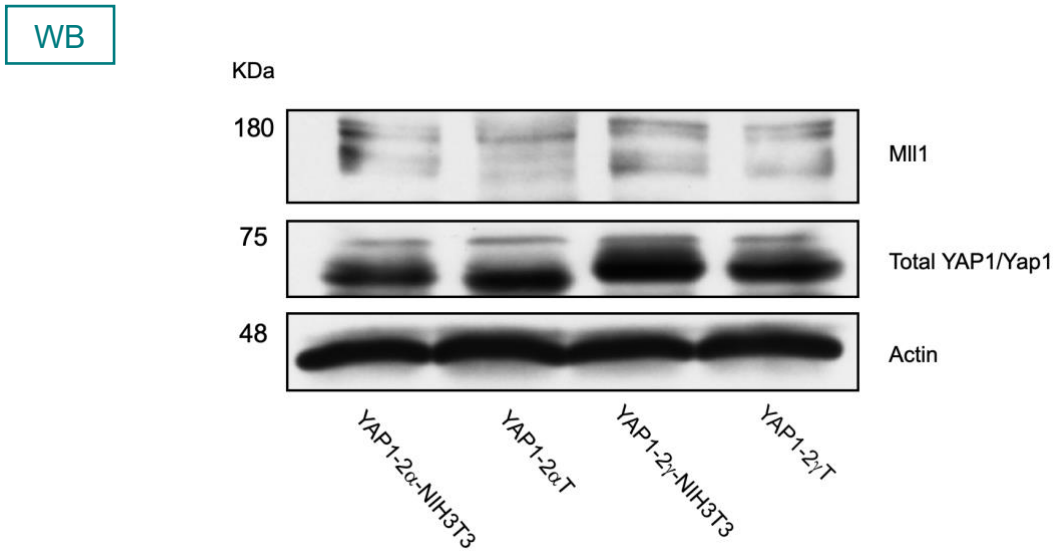

The protein expression levels of *Mll1* in YAP1-2αT, YAP1-2γT, YAP1-2α–NIH3T3 and YAP1-2γ–NIH3T3.

C

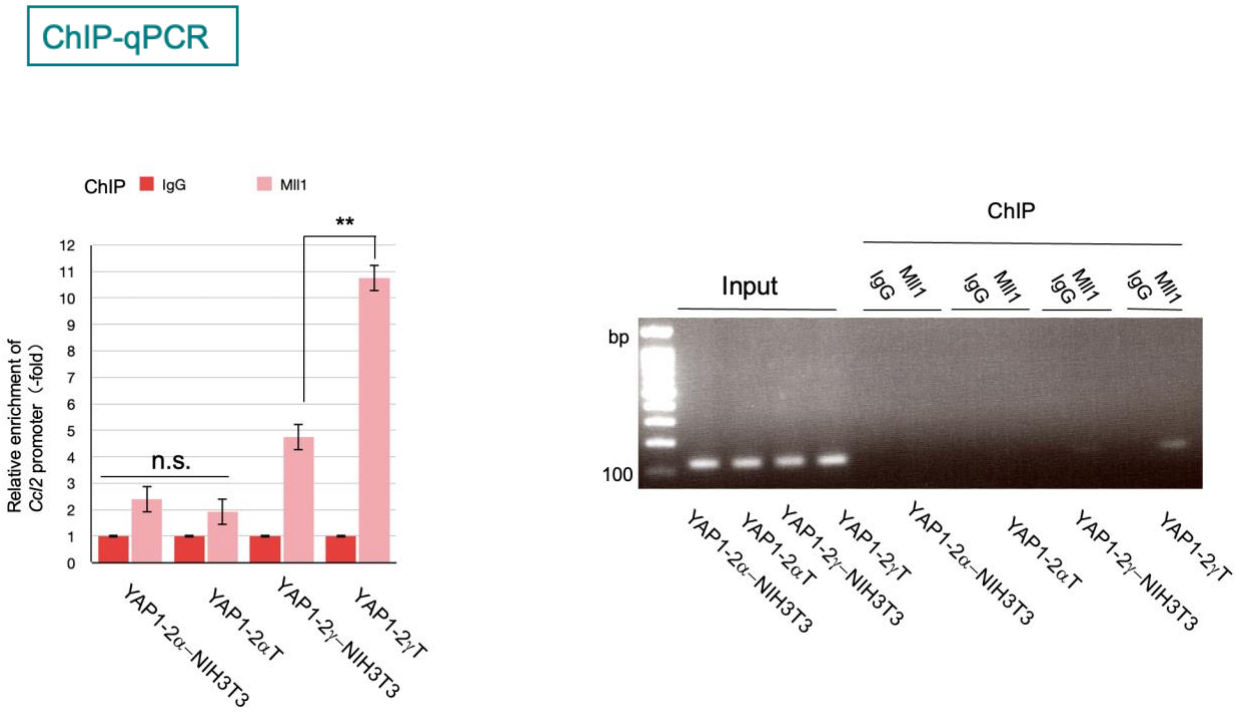

The ChIP analysis (anti-Mll1) of YAP1-2αT, YAP1-2γT, YAP1-2α–NIH3T3 and YAP1-2γ–NIH3T3.

Figure 4. Accumulation of the histone methyltransferase Mll1 at *Ccl2* promoter in YAP1-2γT cells. A. Chromatin was prepared from YAP1-2αT, YAP1-2γT, YAP1-2α–NIH3T3 and YAP1-2γ–NIH3T3 cells fixed with formaldehyde. The ChIP analysis were performed with anti-H3K4me3 antibody or control anti-rabbit IgG antibody. The primer set which target the *Ccl2*$^{-1040\ bp/-950\ bp}$ promoter region were used to quantified fold change. Error bar represents means S.D., **： $p < 0.01$. Student's t-test. Quantitative data were obtained from three independent experiments. B. The expression levels of YAP1/Yap1, Mll1, and Actin in YAP1-2αT cell, YAP1-2γT cells, and YAP1-2α–NIH3T3 and YAP1-2γ–NIH3T3 cells were determined by immunoblot analysis. Cell lysates from YAP1-2αT cell, YAP1-2γT cells, YAP1-2α–NIH3T3 and YAP1-2γ–NIH3T3 cells were subjected to immunoblot analysis with the respective antibodies. C. Chromatin was

prepared from YAP1-2α–NIH3T3, YAP1-2γ–NIH3T3 cells, YAP1-2αT, and YAP1-2γT cells fixed with formaldehyde. The ChIP analysis were performed with anti-Mll1 antibody or control anti-rabbit IgG antibody. The primer set which target the *Ccl2*$^{-1040\ bp/-950\ bp}$ promoter region were used to quantified fold change. Error bars represents means. S.D., **: $p < 0.01$. Student's t-test. Quantitative data were obtained from three independent experiments.

4. Hypoxia increased *Ccl2* expression.

We next investigated the mechanism by which YAP1-2γT cells has greater ability to recruit the Mll1 methyltransferase than YAP1-2αT cells does. ChIP-seq analysis of H3K4me3 status in YAP1-2αT and YAP1-2γT cells revealed that hypoxia-related genes were specifically activated in YAP1-2γT cells (Figure 2C). When combined with the RNA-seq data, we found that several hypoxia-related genes were substantially upregulated in YAP1-2γT cells compared to YAP1-2γ–NIH3T3. The genes included *hypoxia-inducible Factor 1 (Hif1)*, *BCL2 interacting protein 3 (Bnip3)* (29), *DNA damage inducible transcript 4 (Ddit4)* (30), and *insulin-like growth factor binding protein-4 (Igfbp4)* (31) (Figure 5A). The upregulation of *Hif1, Bnip3,* and *Ddit4* were confirmed by qRT-PCR (Figure 5A).

Also, notably, a number of studies indicated the relationship between *CCL2/Ccl2* expression and hypoxia. Chronic hypoxia causes a reduction in the expression of *CCL2* in uveal melanoma (32). On the other hand, hypoxia upregulated the *CCL2* expression level in breast cancer and hepatoma cells (33, 34). Hypoxia has also been reported to crosstalk with YAP1/TAZ in the development of cancer (35, 36).

HIF-1 is a basic helix-loop-helix transcription factor consisting of two DNA binding proteins, HIF-1α and HIF-1β, which play an integral role in the response to hypoxia. Under hypoxia, HIF-1 binds to hypoxia response elements and activates the transcription of target genes (37). As co-activators, YAP1 and TAZ potentiate transactivation of *HIF-1* mRNA in breast cancer cells and hepatoma cells (38). In addition, current studies have shown that *MLL1* is a novel hypoxia response gene, indirectly regulated by the HIF-1 (39). It is therefore possible that hypoxia recruits Mll1 to the *Ccl2* promoter and thereby potentiates Ccl2 transcription in YAP1-2γT cells.

To test this idea, the hypoxia-specific transcription factor Hif-1was induced by treating NIH3T3 cells with cobalt (II) chloride hexahydrate ($CoCl_2$), a chemical inducer of HIF-1/Hif-1 (40). To determine the optimal dose of $CoCl_2$ for NIH3T3 cells, 50 μM, 100 μM, or 150 μM $CoCl_2$ was added to the culture medium. The cell culture was kept for 24 hours in a conventional incubator (37 °C; 5% CO2) (41). Induction of hypoxia was evaluated by the level of Hif-1α with an anti-Hif-1α immunoblotting. As a consequence, both 100 μM, and 150 μM $CoCl_2$ induced Hif-1α in both YAP1-2γT cells and YAP1-2γ–NIH3T3 cells (Figure 5B). At the 100 μM or 150 μM

$CoCl_2$ treatment, YAP1-2γ–NIH3T3 cells showed greater expression of Ccl2 compared to YAP1-2γT cells (Figure 5B). Treatment with 150 μM $CoCl_2$ significantly elevated YAP1 expression, to make YAP1 expression at comparable levels among each sample, the concentration of $CoCl_2$ at 100 μM was chosen for further experiments.

Figure 5

A

RNA-seq

qRT-PCR

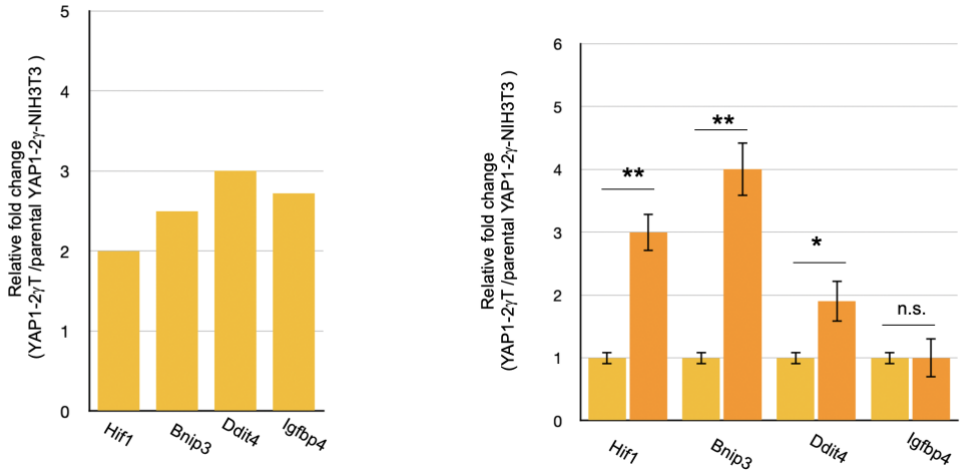

The mRNA expression level of *Hif1*, *Bnip3*, *Ddit4* and *Igfbp4* in YAP1-2γT cells compared with YAP1-2γ–NIH3T3

B

WB

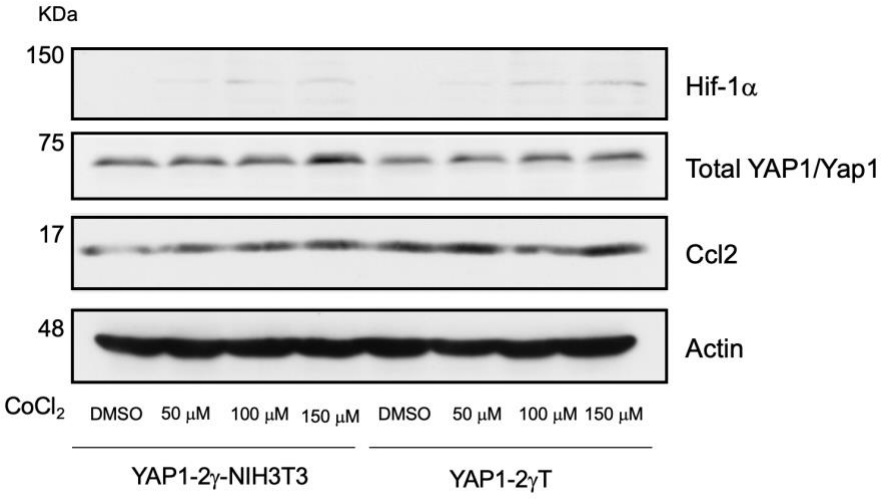

The protein expression levels of *Ccl2* in YAP1-2γ–NIH3T3 and YAP1-2γT under the $CoCl_2$ treatment.

Figure 5. Hypoxia increased Ccl2 expression. A. The mRNA expression level of *Hif1*, *Bnip3*, *Ddit4* were higher in YAP1-2γT cells compared with YAP1-2γ–NIH3T3. Quantitative data were obtained from three independent experiments. B. The expression levels of Hif1α, total YAP1/Yap1, Ccl2, and Actin were determined by immunoblot analysis. Cell lysates from 50 μM, 100 μM, or 150 μM $CoCl_2$ or DMSO treated YAP1-2γT cells or YAP1-2γ–NIH3T3 were subjected to immunoblot analysis with the respective antibodies.

5. Hypoxia induced the enrichment of H3K4me3 and Mll1.

To examine H3K4 modification of the *Ccl2* promoter under hypoxia, a ChIP-qPCR analysis was performed with the anti-H3K4me3 antibody. A marked increase in the level of H3K4me3 was detected after 24 hours of Hif-1 induction at the *Ccl2* promoter region in YAP1-2γ–NIH3T3 cells (Figure 6A). Elevated H3K4me3 was also observed in YAP1-2γT cells, but the change was not as significant as that shown in YAP1-2γ–NIH3T3 cells, most probably due to YAP1-2γT cells maintaining a highly methylated state (Figure 6A). Accordingly, the epigenetic changes reflected the levels of Mll1 at the *Ccl2* promoters in each cell. Under Hif-1 induction, a greater increase in Mll1 at the *Ccl2* promoters was shown in the YAP1-2γ–NIH3T3 cells than in the YAP1-2γT cells (Figure 6B).

To investigate if the recruitment of Mll1 is responsible for the *Ccl2* up-regulation induced by Hif-1α, a Menin-MLL inhibitor MI-2 was used to treat YAP1-2γ–NIH3T3 cells and YAP1-2γT cells 24 hours before Hif-1α induction (42). Menin is a core component for MLL1/2 histone methyltransferases complex, although the detailed role of menin in these complexes is remain unclear, many studies revealed that menin is required for the methyltransferase activity of

MLL1 and MLL2 via promoting their recruitment to target genes and facilitating the interaction between MLL1/2 and other histone methyltransferase complex component (43, 44, 45).

ChIP-qPCR revealed that under the MI-2 treatment, the recruitment of Mll1 induced by Hif-1α was impeded (Figure 6C). Moreover, the up-regulation of Ccl2 induced by Hif-1α was revoked in YAP1-2γ–NIH3T3 cells, suggesting that Mll1 recruitment is essential for the Ccl2 induction triggered by Hif-1α (Figure 6D).

To consolidate previous result that Hif-1α triggered the H3K4me3 at *Ccl2* promoters by recruiting Mll1, Hif-1α knockdown experiments were performed in YAP1-2γ–NIH3T3 cells and YAP1-2γT cells by using two specific siRNA ($Hif\text{-}1\alpha^{KD}$ #1 and $Hif\text{-}1\alpha^{KD}$ #2) or control siRNA. Western blot data showed that $Hif\text{-}1\alpha^{KD}$ #2 siRNA markedly decreased the Hif-1α induction under the $CoCl_2$ treatment, which was concomitantly associated with the inhibition of the Ccl2 elevation (Figure 6E). Moreover, knock down of Hif-1α by $Hif\text{-}1\alpha^{KD}$ #2 siRNA diminished the recruitment of Mll1 at the *Ccl2* promoters in YAP1-2γ–NIH3T3 cells and YAP1-2γT cells indicating that Hif-1α play a vital role in the enhancement of Ccl2 expression through recruiting Mll1 (Figure 6F). Altogether, these results indicated that YAP1-2γ–NIH3T3

cells responded to hypoxia more sensitively and thereby elevated H3K4me3 at *Ccl2* promoters by recruiting Mll1.

Figure 6

A

ChIP-qPCR

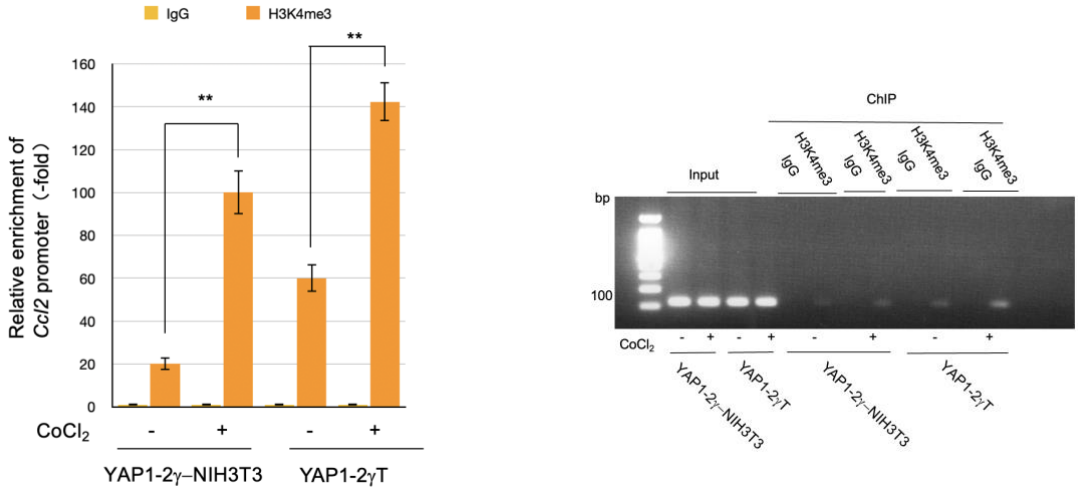

The ChIP analysis (anti-H3K4me3) of YAP1-2γ–NIH3T3 αnd YAP1-2γT under the under the $CoCl_2$ treatment.

B

ChIP-qPCR

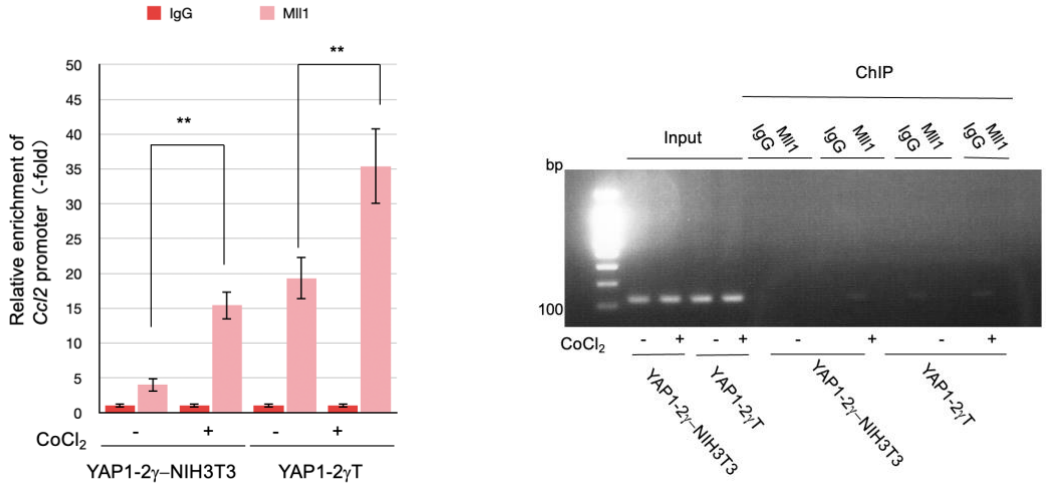

The ChIP analysis (anti-Mll1) of YAP1-2γ–NIH3T3 and YAP1-2γT under the $CoCl_2$ treatment.

C

ChIP-qPCR

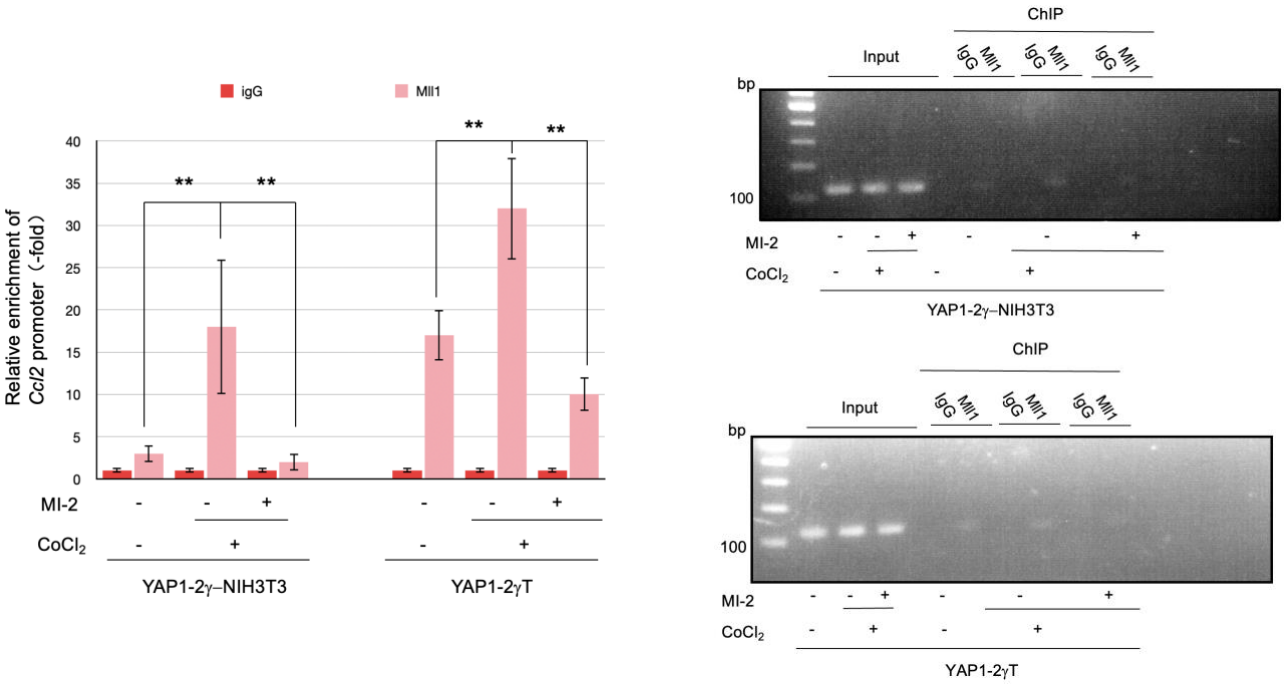

The ChIP analysis (anti-Mll1) of YAP1-2γ–NIH3T3 and YAP1-2γT under the MI-2 treatment.

D

WB

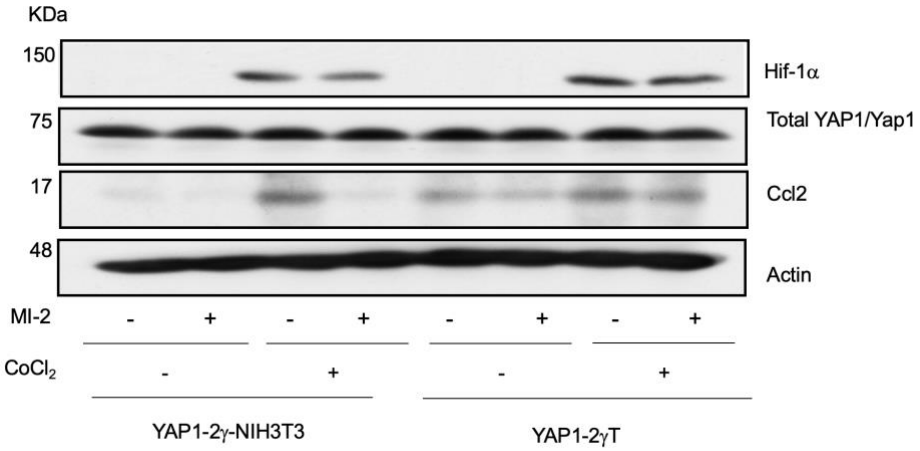

The protein expression levels of *Ccl2* in YAP1-2γ–NIH3T3 and YAP1-2γT under the MI-2 treatment.

E

WB

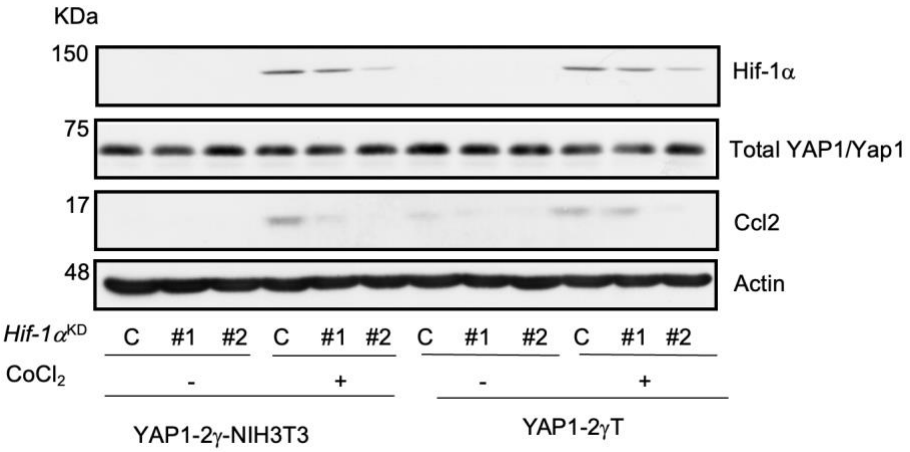

The protein expression levels of *Ccl2* in YAP1-2γ–NIH3T3 and YAP1-2γT under the *Hif-1α* knockdown.

F

ChIP-qPCR

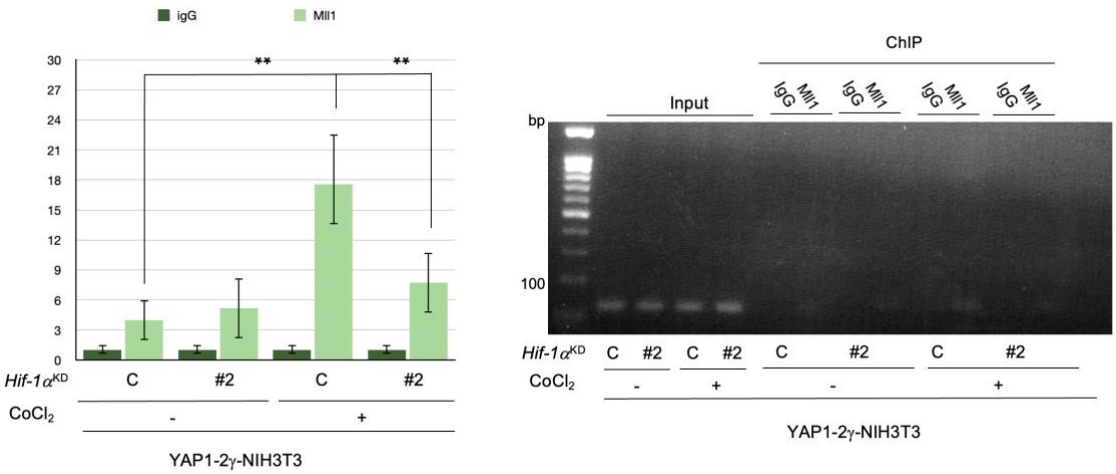

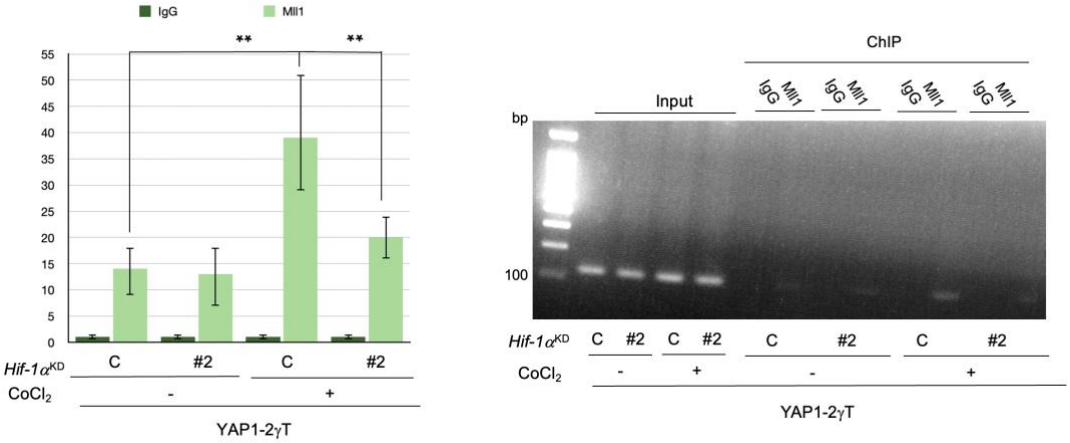

The ChIP analysis (anti-Mll1) of YAP1-2γ–NIH3T3 and YAP1-2γT under the *Hif-1α* knockdown.

Figure 6. Hypoxia promotes the accumulation of Mll1 H3K4me3 methyltransferase to the *Ccl2* promoter. A. Chromatin was prepared from 100μM $CoCl_2$ or DMSO treated YAP1-2γ–NIH3T3, and YAP1-2γT cells fixed with formaldehyde. The ChIP analysis were performed with anti-H3K4me3 antibody or control anti-rabbit IgG antibody. The primer set which target the *Ccl2*$^{-1040\ bp/-950\ bp}$ promoter region were used to quantified fold change. Error bars represents means S.D., **：$p < 0.01$. Student's t-test. Quantitative data were obtained from three independent experiments. B. Chromatin was prepared from 100μM Cobalt (II) Chloride hexahydrate or DMSO treated YAP1-2γ–NIH3T3 and YAP1-2γT cells fixed with formaldehyde. The ChIP analysis were performed with anti-Mll1 antibody or control anti-rabbit IgG antibody. The primer set which target the *Ccl2*$^{-1040\ bp/-950\ bp}$ promoter region were used to quantified fold change. Error bars represents means. S.D., **: $p < 0.01$. Student's t-test. Quantitative data were obtained from three independent experiments. C. Cells were treated with MI-2 for 24 hours. Chromatin was prepared from 100μM Cobalt (II) Chloride hexahydrate or DMSO treated YAP1-2γ–NIH3T3 and YAP1-2γT cells fixed with formaldehyde. The ChIP analysis were performed with anti-Mll^{c180} antibody or control anti-rabbit IgG antibody. The primer set which target the *Ccl2*$^{-1040\ bp/-950\ bp}$ promoter region were used to quantified fold change. Error bars represents means. S.D., **: $p < 0.01$. Student's t-test. Quantitative data were obtained from three independent experiments. D. The expression levels of Hif1α, total YAP1/Yap1, Ccl2, and Actin were determined by immunoblot analysis. Cells were

treated with MI-2 for 24 hours. Cell lysates from 100 μM $CoCl_2$ or DMSO treated YAP1-2γT cells or YAP1-2γ–NIH3T3 were subjected to immunoblot analysis with the respective antibodies. E. The expression levels of Hif1α, total YAP1/Yap1, Ccl2, and Actin were determined by immunoblot analysis. YAP1-2γT cells or YAP1-2γ–NIH3T3 were transfected two specific siRNA ((*Hif-1α*^{KD} #1 and *Hif-1α*^{KD} #2) or control RNA. And then cells were treated with 100 μM $CoCl_2$ or DMSO. Lysates from $CoCl_2$ or DMSO treated YAP1-2γT cells or YAP1-2γ–NIH3T3 were subjected to immunoblot analysis with the respective antibodies. F. Cells were transfected with *Hif-1α*^{KD} #2 for 24 hours. Chromatin was prepared from 100μM Cobalt (II) Chloride hexahydrate or DMSO treated YAP1-2γ–NIH3T3 and YAP1-2γT cells fixed with formaldehyde. The ChIP analysis were performed with anti-Mll1 antibody or control anti-rabbit IgG antibody. The primer set which target the *Ccl2*$^{-1040\ bp/-950\ bp}$ promoter region were used to quantified fold change. Error bars represents means. S.D., **: $p < 0.01$. Student's t-test. Quantitative data were obtained from three independent experiments.

6. Hif-1α induced greater increases in Ccl2 in YAP1-2γ–expressing cells than in YAP1-2α–expressing cells

To corroborate the conclusion that hypoxia modifies Ccl2 expression in NIH3T3 cells expressing YAP1 isoforms, YAP1-2α–NIH3T3, YAP1-2αT, YAP1-2γ–NIH3T3, and YAP1-2γT cells were treated with 100 μM $CoCl_2$ for 24 hours. All the cells treated with $CoCl_2$ induced Hif-1α. Like the case of previous study, YAP1-2γ–NIH3T3 cells induced greater Ccl2 than YAP1-2γT cells did. Interestingly, under the $CoCl_2$ treatment, no change was observed in the level of Ccl2 in YAP1-2α–NIH3T3 transfectants or YAP1-2αT cells (Figure 7A).

In our previous study, we constructed *Yap1*-knockout NIH3T3 cells ($Yap1^{KO}$ NIH3T3) by using the CRISPR–Cas9 system. Then, $Yap1^{KO}$ NIH3T3 cells were transfected with vectors expressing sgRNA-resistant HA-YAP1-2α or HA-YAP1-2γ to generate $Yap1^{KO}$-2α NIH3T3 cells and $Yap1^{KO}$-2γ NIH3T3 cells, respectively (17).

To consolidate previous result that YAP1-2α and YAP1-2γ exhibited different response to hypoxia, Hif-1 induction experiment was performed by using NIH3T3 cells, *Yap1*^{KO}-2α NIH3T3 cells and *Yap1*^{KO}-2γ NIH3T3 cells. Consistently, under the 100 μM $CoCl_2$ treatment, dramatical upregulation of Ccl2 was detected in *Yap1*^{KO}-2γ NIH3T3 cells. In contrast, no change was observed in the level of Ccl2 in NIH3T3 cells and *Yap1*^{KO}-2α NIH3T3 cells upon Hif1 induction (Figure 7B). These results indicated that the response to hypoxia can be driven in YAP1 isoforms-specific manner.

Figure 7

A

WB

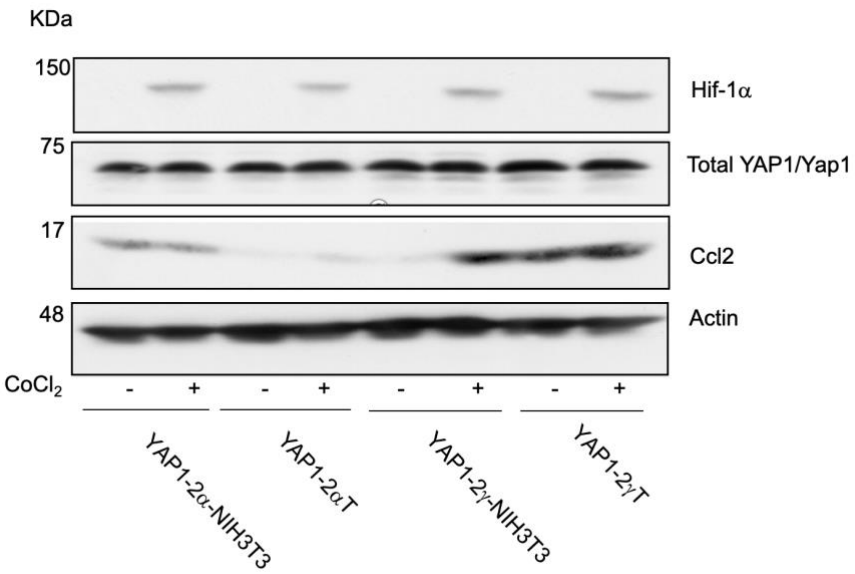

The protein expression levels of *Ccl2* in YAP1-2αT, YAP1-2γT, YAP1-2α–NIH3T3 and YAP1-2γ–NIH3T3 under the $CoCl_2$ treatment.

B

WB

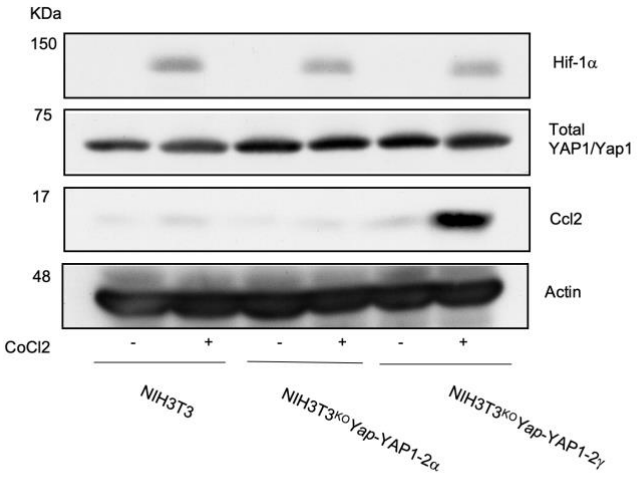

The protein expression levels of *Ccl2* in NIH3T3, NIH3T3^{ko}*Yap*-YAP1-2α, and NIH3T3^{ko}*Yap*-YAP1-2γ under the $CoCl_2$ treatment.

Figure 7. Hypoxia induced more significant increases in Ccl2 in YAP1-2γ–expressing cells than YAP1-2α–expressing cells. A. The expression levels of Hif1α, total YAP1/Yap1, Ccl2, and Actin were determined by immunoblot analysis. Cell lysates from 100 μM $CoCl_2$ or DMSO treated YAP1-2α–NIH3T3, YAP1-2αT, YAP1-2γ–NIH3T3, and YAP1-2γT were subjected to immunoblot analysis with the respective antibodies. B. The expression levels of Hif1α, total YAP1/Yap1, Ccl2, and Actin were determined by immunoblot analysis. Cell lysates from 100 μM $CoCl_2$ or DMSO treated NIH3T3 cells, $Yap1^{KO}$-2α NIH3T3 cells, and $Yap1^{KO}$-2γ NIH3T3 cells were subjected to immunoblot analysis with the respective antibodies.

Discussion

1. Summary

Previously, we demonstrated that YAP1-2γ exhibits greater *in vitro* pro-oncogenic potential and shows stronger mitogenic and motogenic activities than YAP1-2α does. Mechanistically, YAP1-2γ exhibits stronger cell-intrinsic prooncogenic activity because SHP2, which is retained in the cytoplasm without binding YAP1-2, potentiates RAS–ERK signaling, thereby promoting cell proliferation and motility. (17).

Conversely, YAP1-2γ displayed a substantially weaker *in vivo* tumorigenicity than YAP1-2α by establishing microenvironments that impairs tumorigenicity in a non-cell-autonomous mechanism. The nuclear YAP1-2γ/Tead complex efficiently transactivates *Ccl2*, whereas YAP1-2α, which binds to SHP2, formed a heterodimeric complex with Tead in the nucleus, which repressed rather than promoted *Ccl2* transcription (17).

Furthermore, the YAP1-2γ/Tead complex stimulated *Ccl2* in response to hypoxia, which represents *in vivo* situation. In YAP1-2γ expressing cells, Hif-1α induced H3K4me3-mediated

upregulation of Ccl2 by recruiting methyltransferase Mll1 to the *Ccl2* promoter region (Figure 8A). The elevated expression of proinflammatory cytokine Ccl2 triggered the recruitment of tumor-inhibitory macrophages to areas with chronic hypoxia, which consequently created a "hot" tumor microenvironment. On the other hand, YAP1-2α, which does not respond to hypoxia, functions as a transrepressor of *Ccl2* by forming the YAP1-2α/Tead/SHP2 heterotrimeric complex, which dampens macrophage accumulation and derives the "cold" tumor microenvironment (Figure 8B).

Interestingly, the histopathological examination revealed massive infiltration of F4/80- positive macrophages in the center of the YAP1-2γ-driven tumors. However, in YAP1-2α–driven tumors, macrophages infiltrated at the boundary of tumor (Figure 8C). This result supporting our conclusion that during the growth of the tumor, chronic hypoxia occurs in the center of the tumor, YAP1-2γ triggered the recruitment of macrophages to areas with hypoxia by upregulating *Ccl2*.

Figure 8

A

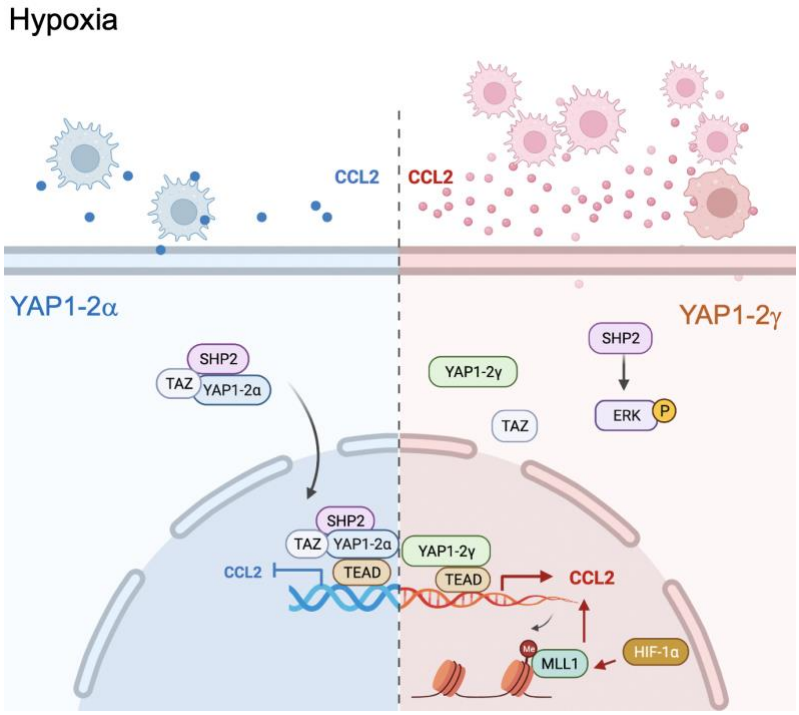
Hypoxia
CCL2
CCL2
YAP1-2α
YAP1-2γ
SHP2
TAZ
YAP1-2α
YAP1-2γ
SHP2
ERK
P
TAZ
SHP2
TAZ
YAP1-2α
YAP1-2γ
CCL2
TEAD
TEAD
CCL2
Me
MLL1
HIF-1α

B

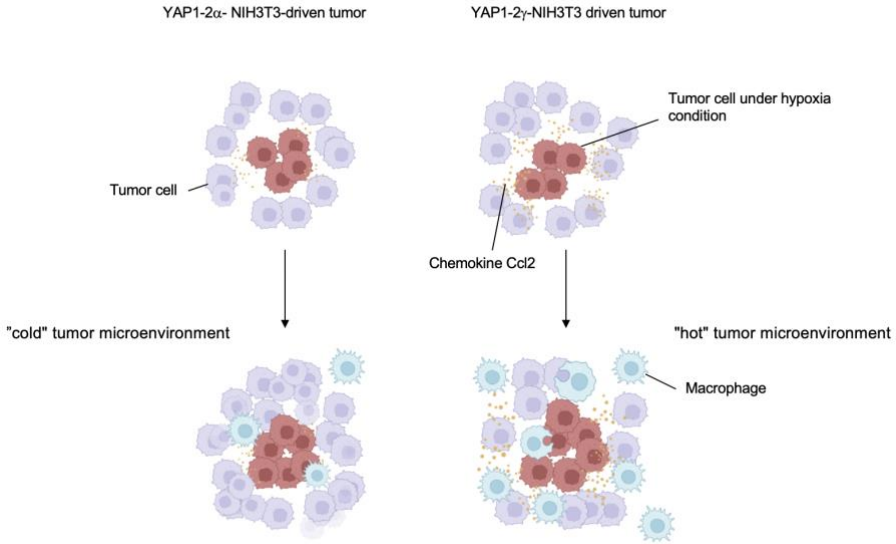

C

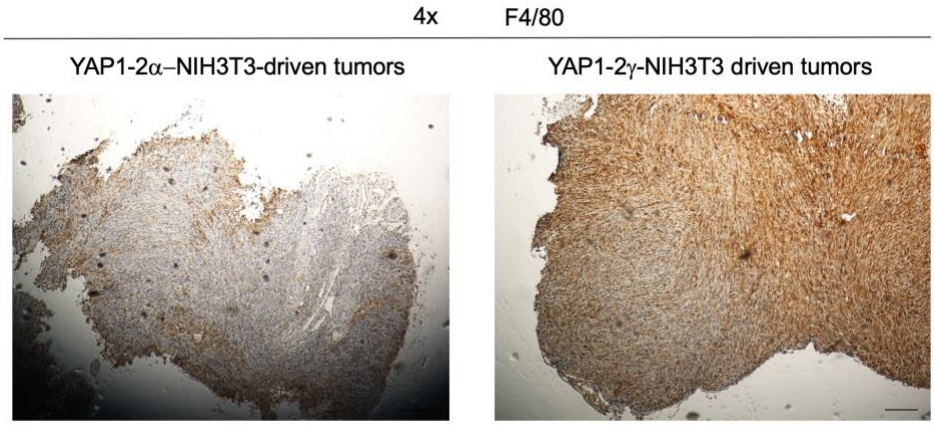

Figure 8. Summary. A. Alternative splicing influences the cell-intrinsic and cell-extrinsic prooncogenic activities of YAP1. B. Alternative tumor microenvironment generated by differentially spliced YAP1 isoforms. C. Formalin-fixed and paraffin-embedded serial sections of the YAP1-2γ-NIH3T3 driven tumor and YAP1-2α–NIH3T3 driven tumor tissues were stained with an anti-F4/80 antibody. *Scale bars*, 200 μm.

2. The crosstalk between YAP1, MLL1 and hypoxia.

In this work, I found that YAP1/TAZ associate with the histone methyltransferase complex to alter epigenetic modifications, thereby affecting target gene activation. The *de novo* state of chromatin analysis revealed that organoids derived from human colorectal cancer patients (PDOs) detected active enhancer sites, marked by enriched H3K27ac and H3k4me3. Such CRC enhancerome are in most cases regulated by YAP1/TAZ, suggesting that the transcriptional coactivators serve as critical players in the epigenetic deregulation of gene expression in CRCs (46). Consistently, Heuberger et al. showed that Yap1 interacts with the histone-methyltransferase complex component Mll1 and WD repeat domain 5 (Wdr5) (27). Although the structures of YAP1 and TAZ proteins are well elucidated, it remains still unclear if YAP1/TAZ can directly interact with MLL1. Thus, the mode of interaction MLL1 and YAP1-2α or YAP1-2γ needs further investigation.

Analysis of the TCGA database revealed a significant positive correlation between YAP1 and MLL1 in breast cancer, hepatocellular carcinoma, colon cancer, and stomach cancer. These clinical data also point to the functional interplay between YAP1 and MLL1, probably in

perturbing epigenetic regulation of transcriptional network by perturbing H3K4me3-refulated gene regulation (47) (Figure 9A).

Hypoxia, one of the most frequent and severe environmental stresses to homeostatic mechanisms *in vivo*, is a state of insufficient oxygen availability. Hypoxia-mediated responses are highly integrated across many diseases, including cancer (48). Recent studies suggest that chronic hypoxia plays an initial role in inducing DNA methylation, demethylation, and/or histone modifications (49). Indeed, the histone methylation is significantly modified under hypoxia. For example, Batie et al. detected a rapid and robust increase in H3K4me3 in HeLa cells within 30 min of hypoxia exposure (50).

So far, however, there is limited information whether specific methyltransferase can be recruited or elevated under hypoxic condition. Heddleston et al. first demonstrated that *MLL1* is a hypoxia-responsive gene, the expression level of which can be increased in glioma stem cells by hypoxia-activated HIF-1α and HIF-2α (51). Moreover, a recent study revealed that one of the (MLL)/SET methyltransferase family members—SET1B, can be recruited to chromatin under hypoxia in HEK293T cells (52). In this work, I demonstrated an unprecedented

connection between YAP1-2γ, Hif-1α, and H3K4me3 methyltransferase Mll1, which transactivates the *Ccl2* promoter in cells predominantly expressing YAP1-2γ. It is possible that YAP1-2γ, HIF-1α, and MLL1 could form a complex in cells, which bind to the TEAD and effect TEAD target gene expression. Other TEAD target genes other than *CCL2* may also be regulated by similar mechanisms in response to oxygen concentrations *in vivo* (Figure 9B).

Figure 9

A

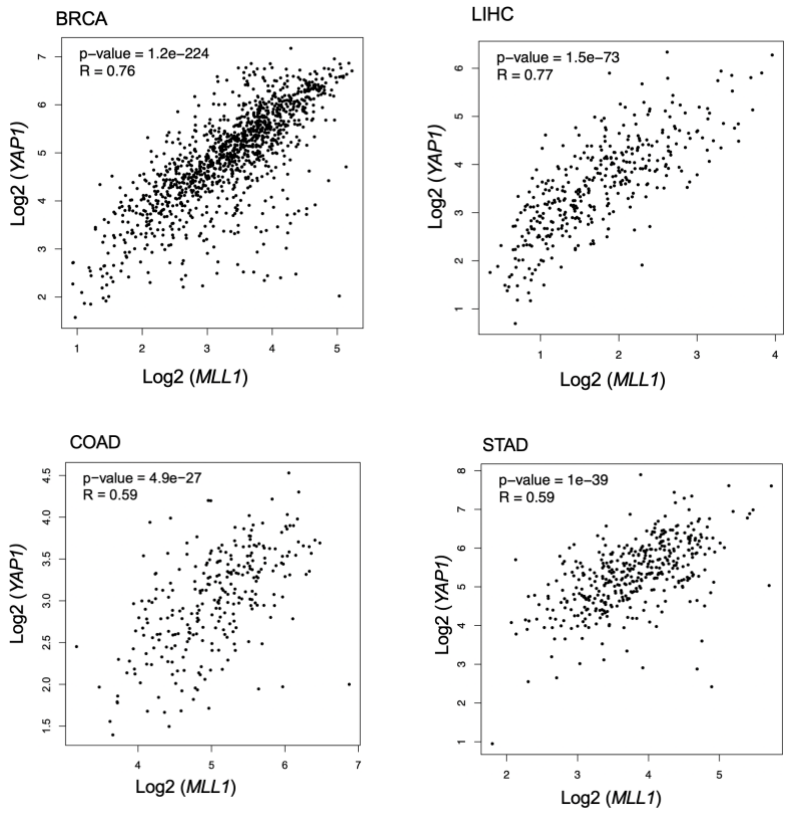

B

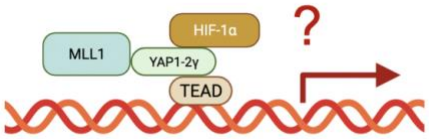

Figure 9. The co-expression analysis of *YAP1* and *MLL1*. A. The expression of *MLL1* is strongly positively correlated with *YAP1* in patients of BRCA, LIHC, COAD, and STAD. The co-expression data is obtained from GEPIA2 based on TCGA and GTEx data (53). Correlation coefficient: Spearman. B. The hypothesis of the crosstalk between YAP1-2γ, MLL1 and HIF-1α.

3. The response to hypoxia was intrinsically driven in a manner that is dependent on YAP1 isoforms.

Mechanism underlying hypoxia increased *Ccl2* expression much more significant in YAP1-2γ–expressing cells than in YAP1-2α–expressing cells remains unclear.

Hypoxia is a central pathological stimulus that regulates the transcription of genes (53). Under hypoxia, changes in chromatin accessibility which allows the access to DNA, are essential for the cellular processes (54). In our study, hypoxia induces open chromatin structure in the *Ccl2* promoter, making the YAP1-2γ/Tead transactivate complex easily accessible, thereby potentiating *Ccl2* mRNA and protein expression. On the other hand, the YAP1-2α/Tead/SHP2 complex may also become more accessible to *Ccl2* promoter under hypoxia. However, this heterotrimeric complex acts as the repressor rather than the activator, thereby downregulating *Ccl2/CCL2* expression.

4.The limitation of this study.

Limitation of study example should be noted here. Previously, we used 5 pairs (pair 1-5) of the NIH3T3 transfectants to performed allograft transplantation experiments. In present study, single pair (from pair 5) *in vitro* cell lines were successfully re-established from tumors developed by YAP1-2α–NIH3T3 cells or YAP1-2γ–NIH3T3 in nude mice.

It is risky to conclude our mechanism by using single pair of cell line. For example, during the tumor formation, the mixtures of passenger and driver mutations may occur in cancer genomes [55]. Each individual tumor will exhibit a unique combination of mutations; thus, specific molecular mechanism may be involved in such case. The analysis of independent cell lines from the same transfectants-driven tumors and cell lines re-established from other NIH3T3 transfectants-driven tumors may help to confirm the conclusion.

Reference

1. Zhao, B., Wei, X., Li, W., Udan, R. S., Yang, Q., Kim, J., ... & Guan, K. L. (2007). Inactivation of YAP oncoprotein by the Hippo pathway is involved in cell contact inhibition and tissue growth control. *Genes & development*, 21(21), 2747-2761.

2. Pan, D. (2007). Hippo signaling in organ size control. Genes & development, 21(8), 886-897.

3. Schlegelmilch, K., Mohseni, M., Kirak, O., Pruszak, J., Rodriguez, J. R., Zhou, D., ... & Camargo, F. D. (2011). Yap1 acts downstream of α-catenin to control epidermal proliferation. Cell, 144(5), 782-795.

4. Freeman, A. K., & Morrison, D. K. (2011, September). 14-3-3 Proteins: diverse functions in cell proliferation and cancer progression. In Seminars in cell & developmental biology (Vol. 22, No. 7, pp. 681-687). Academic Press.

5. Zanconato, F., Cordenonsi, M., & Piccolo, S. (2016). YAP/TAZ at the roots of cancer. *Cancer cell*, 29(6), 783-803.

6. Zhao, B., Ye, X., Yu, J., Li, L., Li, W., Li, S., ... & Guan, K. L. (2008). TEAD mediates YAP-dependent gene induction and growth control. *Genes & development*, *22*(14), 1962-1971.

7. Dong, J., Feldmann, G., Huang, J., Wu, S., Zhang, N., Comerford, S. A., ... & Pan, D. (2007). Elucidation of a universal size-control mechanism in Drosophila and mammals. *Cell*, *130*(6), 1120-1133.

8. Cai, J., Zhang, N., Zheng, Y., De Wilde, R. F., Maitra, A., & Pan, D. (2010). The Hippo signaling pathway restricts the oncogenic potential of an intestinal regeneration program. *Genes & development*, *24*(21), 2383-2388

9. Gaffney, C. J., Oka, T., Mazack, V., Hilman, D., Gat, U., Muramatsu, T., ... & Sudol, M. (2012). Identification, basic characterization and evolutionary analysis of differentially spliced mRNA isoforms of human YAP1 gene. *Gene*, 509(2), 215-222.

10. Sudol, M. (2013). YAP1 oncogene and its eight isoforms. *Oncogene*, 32(33), 3922-3922

11. Liu, X., & Qu, C. K. (2011). Protein tyrosine phosphatase SHP-2 (PTPN11) in hematopoiesis and leukemogenesis. *Journal of signal transduction*, 2011.

12. Hatakeyama, M. (2014). Helicobacter pylori CagA and gastric cancer: a paradigm for hit-and-run carcinogenesis. *Cell host & microbe*, 15(3), 306-316.

13. Tsutsumi, R., Masoudi, M., Takahashi, A., Fujii, Y., Hayashi, T., Kikuchi, I., ... & Hatakeyama, M. (2013). YAP and TAZ, Hippo signaling targets, act as a rheostat for nuclear SHP2 function. *Developmental cell*, 26(6), 658-665.

14. Chan, G., Kalaitzidis, D., & Neel, B. G. (2008). The tyrosine phosphatase Shp2 (PTPN11) in cancer. *Cancer and metastasis reviews*, 27(2), 179-192.

15. Dance, M., Montagner, A., Salles, J. P., Yart, A., & Raynal, P. (2008). The molecular functions of Shp2 in the Ras/Mitogen-activated protein kinase (ERK1/2) pathway. *Cellular signalling*, 20(3), 453-459.

16. Liu, J. J., Li, Y., Chen, W. S., Liang, Y., Wang, G., Zong, M., ... & Feng, G. S. (2018). Shp2 deletion in hepatocytes suppresses hepatocarcinogenesis driven by oncogenic β-Catenin, PIK3CA and MET. *Journal of hepatology*, 69(1), 79-88.

17. Ben, C., Wu, X., Takahashi-Kanemitsu, A., Knight, C. T., Hayashi, T., & Hatakeyama, M. (2020). Alternative splicing reverses the cell-intrinsic and cell-extrinsic pro-oncogenic potentials of YAP1. *Journal of Biological Chemistry*, 295(41), 13965-13980.

18. Zhu, J., Adli, M., Zou, J. Y., Verstappen, G., Coyne, M., Zhang, X., ... & Bernstein, B. E. (2013). Genome-wide chromatin state transitions associated with developmental and environmental cues. *Cell*, 152(3), 642-654.

19. Michalak, E. M., Burr, M. L., Bannister, A. J., & Dawson, M. A. (2019). The roles of DNA, RNA and histone methylation in ageing and cancer. *Nature reviews Molecular cell biology,* 20(10), 573-589.

20. Xu, B., Li, S. H., Zheng, R., Gao, S. B., Ding, L. H., Yin, Z. Y., ... & Jin, G. H. (2013). Menin promotes hepatocellular carcinogenesis and epigenetically upregulates Yap1 transcription. *Proceedings of the National Academy of Sciences*, 110(43), 17480-17485.

21. Della Chiara, G., Gervasoni, F., Fakiola, M., Godano, C., D'Oria, C., Azzolin, L., ... & Pagani, M. (2021). Epigenomic landscape of human colorectal cancer unveils an aberrant core of pan-cancer enhancers orchestrated by YAP/TAZ. *Nature communications*, 12(1), 1-18.

22. Kamps, R., Brandão, R. D., Bosch, B. J., Paulussen, A. D., Xanthoulea, S., Blok, M. J., & Romano, A. (2017). Next-generation sequencing in oncology: genetic diagnosis, risk prediction and cancer classification. *International journal of molecular sciences*, 18(2), 308.

23. Thomas-Chollier, M., Herrmann, C., Defrance, M., Sand, O., Thieffry, D., & van Helden, J. (2012). RSAT peak-motifs: motif analysis in full-size ChIP-seq datasets. *Nucleic acids research*, *40*(4), e31-e31.

24. Subramanian, A., Tamayo, P., Mootha, V. K., Mukherjee, S., Ebert, B. L., Gillette, M. A., ... & Mesirov, J. P. (2005). Gene set enrichment analysis: a knowledge-based approach for

interpreting genome-wide expression profiles. *Proceedings of the National Academy of Sciences*, *102*(43), 15545-15550.

25. Liberzon, A., Subramanian, A., Pinchback, R., Thorvaldsdóttir, H., Tamayo, P., & Mesirov, J. P. (2011). Molecular signatures database (MSigDB) 3.0. *Bioinformatics*, *27*(12), 1739-1740.

26. Hsieh, J. J. D., Ernst, P., Erdjument-Bromage, H., Tempst, P., & Korsmeyer, S. J. (2003). Proteolytic cleavage of MLL generates a complex of N-and C-terminal fragments that confers protein stability and subnuclear localization. *Molecular and cellular biology*, 23(1), 186-194.

27. Heuberger, J., Grinat, J., Kosel, F., Liu, L., Kunz, S., Vidal, R. O., ... & Birchmeier, W. (2021). High Yap and Mll1 promote a persistent regenerative cell state induced by Notch signaling and loss of p53. *Proceedings of the National Academy of Sciences*, 118(22).

28. Hsieh, J. J. D., Ernst, P., Erdjument-Bromage, H., Tempst, P., & Korsmeyer, S. J. (2003). Proteolytic cleavage of MLL generates a complex of N-and C-terminal fragments that confers protein stability and subnuclear localization. *Molecular and cellular biology*, 23(1), 186-194.

29. Bellot, G., Garcia-Medina, R., Gounon, P., Chiche, J., Roux, D., Pouysségur, J., & Mazure, N. M. (2009). Hypoxia-induced autophagy is mediated through hypoxia-inducible factor induction of BNIP3 and BNIP3L via their BH3 domains. *Molecular and cellular biology*, 29(10), 2570-2581

30. Tirado-Hurtado, I., Fajardo, W., & Pinto, J. A. (2018). DNA damage inducible transcript 4 gene: the switch of the metabolism as potential target in cancer. *Frontiers in oncology*, 8, 106.

31. Minchenko, D. O., Kharkova, A. P., Halkin, O. V., Karbovskyi, L. L., & Minchenko, O. H. (2016). Effect of hypoxia on the expression of genes encoding insulin-like growth factors and some related proteins in U87 glioma cells without IRE1 function. *Endocrine regulations*, 50(2), 43-54.

32. Bronkhorst, I. H., Jehs, T. M., Dijkgraaf, E. M., Luyten, G. P., van der Velden, P. A., van der Burg, S. H., & Jager, M. J. (2014). Effect of hypoxic stress on migration and characteristics of monocytes in uveal melanoma. *JAMA ophthalmology*, *132*(5), 614-621.

33. Tripathi, C., Tewari, B. N., Kanchan, R. K., Baghel, K. S., Nautiyal, N., Shrivastava, R., ... & Bhadauria, S. (2014). Macrophages are recruited to hypoxic tumor areas and acquire a pro-angiogenic M2-polarized phenotype via hypoxic cancer cell derived cytokines Oncostatin M and Eotaxin. *Oncotarget*, *5*(14), 5350.

34. Konishi, H., Shirabe, K., Nakagawara, H., Harimoto, N., Yamashita, Y. I., Ikegami, T., ... & Maehara, Y. (2015). Suppression of silent information regulator 1 activity in noncancerous tissues of hepatocellular carcinoma: Possible association with non-B non-C hepatitis pathogenesis. *Cancer science*, *106*(5), 542-549.

35. Zhou TY, Zhuang LH, Hu Y, Zhou YL, Lin WK, Wang DD, et al. Inactivation of hypoxia-induced YAP by statins overcomes hypoxic resistance to sorafenib in hepatocellular carcinoma cells. *Sci Rep*, 2016;6:30483.

36. Xiang L, Gilkes DM, Hu H, Takano N, Luo W, Lu H, et al. Hypoxia-inducible factor 1 mediates TAZ expression and nuclear localization to induce the breast cancer stem cell phenotype. *OncoTarget,* 2014;5: 12509e27.

37. Wang, G. L., Jiang, B. H., Rue, E. A., & Semenza, G. L. (1995). Hypoxia-inducible factor 1 is a basic-helix-loop-helix-PAS heterodimer regulated by cellular O2 tension. *Proceedings of the national academy of sciences*, *92*(12), 5510-5514.

38. Heddleston, J. M., Wu, Q., Rivera, M., Minhas, S., Lathia, J. D., Sloan, A. E., ... & Rich, J. N. (2012). Hypoxia-induced mixed-lineage leukemia 1 regulates glioma stem cell tumorigenic potential. *Cell Death & Differentiation*, *19*(3), 428-439.

39. Heddleston, J. M., Wu, Q., Rivera, M., Minhas, S., Lathia, J. D., Sloan, A. E., ... & Rich, J. N. (2012). Hypoxia-induced mixed-lineage leukemia 1 regulates glioma stem cell tumorigenic potential. *Cell Death & Differentiation*, *19*(3), 428-439.

40. Piret JP, Mottet D, Raes M, Michiels C. CoCl2, a chemical inducer of hypoxia-inducible factor-1, and hypoxia reduce apoptotic cell death in hepatoma cell line HepG2. *Ann N Y Acad Sci*, 2002; 973:443–447

41. Wu, D., & Yotnda, P. (2011). Induction and testing of hypoxia in cell culture. Jo*VE (Journal of Visualized Experiments)*, (54), e2899.

42. Grembecka, J., He, S., Shi, A., Purohit, T., Muntean, A. G., Sorenson, R. J., ... & Cierpicki, T. (2012). Menin-MLL inhibitors reverse oncogenic activity of MLL fusion proteins in leukemia. *Nature chemical biology*, *8*(3), 277-284.

43. Yokoyama, A., Somervaille, T. C., Smith, K. S., Rozenblatt-Rosen, O., Meyerson, M., & Cleary, M. L. (2005). The menin tumor suppressor protein is an essential oncogenic cofactor for MLL-associated leukemogenesis. Cell, 123(2), 207-218.

44. Hughes, C. M., Rozenblatt-Rosen, O., Milne, T. A., Copeland, T. D., Levine, S. S., Lee, J. C., ... & Meyerson, M. (2004). Menin associates with a trithorax family histone methyltransferase complex and with the hoxc8 locus. Molecular cell, 13(4), 587-597.

45. Milne, T. A., Hughes, C. M., Lloyd, R., Yang, Z., Rozenblatt-Rosen, O., Dou, Y., ... & Hess, J. L. (2005). Menin and MLL cooperatively regulate expression of cyclin-dependent kinase inhibitors. *Proceedings of the National Academy of Sciences*, *102*(3), 749-754.

46. Della Chiara, G., Gervasoni, F., Fakiola, M., Godano, C., D'Oria, C., Azzolin, L., ... & Pagani, M. (2021). Epigenomic landscape of human colorectal cancer unveils an aberrant core of pan-cancer enhancers orchestrated by YAP/TAZ. *Nature communications*, 12(1), 1-18.

47. Tang, Z., Li, C., Kang, B., Gao, G., Li, C., & Zhang, Z. (2017). GEPIA: a web server for cancer and normal gene expression profiling and interactive analyses. *Nucleic acids research,* 45(W1), W98-W102.

48. Muz, B., de la Puente, P., Azab, F., & Azab, A. K. (2015). The role of hypoxia in cancer progression, angiogenesis, metastasis, and resistance to therapy. *Hypoxia*, *3*, 83.

49. Ducsay, C. A., Goyal, R., Pearce, W. J., Wilson, S., Hu, X. Q., & Zhang, L. (2018). Gestational hypoxia and developmental plasticity. *Physiological reviews*, *98*(3), 1241-1334.

50. Batie, M., Frost, J., Frost, M., Wilson, J. W., Schofield, P., & Rocha, S. (2019). Hypoxia induces rapid changes to histone methylation and reprograms chromatin. *Science*, *363*(6432), 1222-1226.

51. Heddleston, J. M., Wu, Q., Rivera, M., Minhas, S., Lathia, J. D., Sloan, A. E., ... & Rich, J. N. (2012). Hypoxia-induced mixed-lineage leukemia 1 regulates glioma stem cell tumorigenic potential. *Cell Death & Differentiation*, *19*(3), 428-439.

52. Ortmann, B. M., Burrows, N., Lobb, I. T., Arnaiz, E., Wit, N., Bailey, P. S., ... & Nathan, J. A. (2021). The HIF complex recruits the histone methyltransferase SET1B to activate specific hypoxia-inducible genes. *Nature Genetics*, 1-14.

53. Melvin, A., & Rocha, S. (2012). Chromatin as an oxygen sensor and active player in the hypoxia response. *Cellular signalling*, *24*(1), 35-43.

54. Kindrick, J. D., & Mole, D. R. (2020). Hypoxic regulation of gene transcription and chromatin: Cause and effect. *International Journal of Molecular Sciences*, *21*(21), 8320.

55. Bozic, I., Antal, T., Ohtsuki, H., Carter, H., Kim, D., Chen, S., ... & Nowak, M. A. (2010). Accumulation of driver and passenger mutations during tumor progression. *Proceedings of the National Academy of Sciences*, *107*(43), 18545-18550.

Acknowledgement

I would like to express my deep and sincere gratitude to my research supervisor, Masanori Hatakeyama, for giving me the opportunity to do research and providing invaluable guidance throughout this research. His dynamism, vision, and motivation have deeply inspired me. It was a great privilege and honor to work and study under his guidance. I am extremely grateful for what he has offered me.

In particular, I would like to thank my tutor Dr. Atsushi Takahashi-Kanemitsu for his extraordinary generosity of time and ideas. He has taught me the methodology to carry out the research and to present the research works as clearly as possible.

I would like to offer my humblest thanks to all of the people whose efforts have contributed to this work: Dr. Chi Ben, Dr. Christopher Takaya Knight, and Dr. Takeru Hayashi, prof. Kaneda and all members of the Department of Microbiology.

I am extremely grateful to my parents for their love, prayers, caring, and sacrifices for educating and preparing me for my future. Thanks, Jane and Michael, for their generous support. Also, I express my thanks to my friends. My Special thanks goes to my family members FuFu Feng and cat Ryan for their love and continuing support to my life.

I lost my grandfather on July 2021. Because of the COVID-19, I had no chance to meet him for the last time. I can't get over his death until now; it will be one of the indelible pains of my life.

Xiaojing Wu